

1 **Recognition of microbial viability via TLR8 promotes T follicular helper cell**  
2 **differentiation and vaccine responses**

3 Matteo Ugolini<sup>1\*</sup>, Jenny Gerhard<sup>1\*</sup>, Sanne Burkert<sup>3\*</sup>, Kristoffer Jarlov Jensen<sup>4,5</sup>, Philipp Georg<sup>1</sup>,  
4 Friederike Ebner<sup>6</sup>, Sarah Volkers<sup>1</sup>, Shruthi Thada<sup>3,7</sup>, Kristina Dietert<sup>8</sup>, Laura Bauer<sup>9</sup>, Alexander  
5 Schäfer<sup>10</sup>, Elisa T. Helbig<sup>1</sup>, Bastian Opitz<sup>1,2</sup>, Florian Kurth<sup>1</sup>, Saubashya Sur<sup>3</sup>, Nickel Dittrich<sup>3</sup>,  
6 Sumanlatha Gaddam<sup>7</sup>, J. Magarian Blander<sup>11</sup>, Christine S. Benn<sup>4,12</sup>, Ulrike Blohm<sup>10</sup>, Achim D.  
7 Gruber<sup>8</sup>, Andreas Hutloff<sup>9</sup>, Susanne Hartmann<sup>6</sup>, Mark V. Boekschoten<sup>13</sup>, Michael Müller<sup>13,14</sup>,  
8 Gregers Jungersen<sup>5</sup>, Ralf R. Schumann<sup>3</sup>, Norbert Suttorp<sup>1,2</sup> and Leif E. Sander<sup>1,2</sup>

9 <sup>1</sup>Department of Infectious Diseases and Pulmonary Medicine, Charité – Universitätsmedizin Berlin, corporate member  
10 of Freie Universität Berlin, Humboldt-Universität zu Berlin, and Berlin Institute of Health, Berlin, Germany.

11 <sup>2</sup>German Center for Lung Research (DZL)

12 <sup>3</sup>Institute of Microbiology and Hygiene, Charité University Hospital, Berlin, Germany.

13 <sup>4</sup>Research Center for Vitamins and Vaccines, Bandim Health Project, Statens Serum Institut, Copenhagen S, Denmark

14 <sup>5</sup>Section for Immunology and Vaccinology, National Veterinary Institute, Technical University of Denmark, Kgs  
15 Lyngby, Denmark

16 <sup>6</sup>Department of Veterinary Medicine, Institute of Immunology, Freie Universität Berlin, Berlin, Germany

17 <sup>7</sup>Bhagwan Mahavir Medical Research Centre, Hyderabad, India

18 <sup>8</sup>Department of Veterinary Pathology, Freie Universität Berlin, Berlin, Germany

19 <sup>9</sup>Chronic Immune Reactions, German Rheumatism Research Centre, Berlin, Germany

20 <sup>10</sup>Institute of Immunology, Friedrich-Loeffler-Institut, Federal Research Institute for Animal Health, Greifswald –  
21 Island of Riems, Germany

22 <sup>11</sup>The Jill Roberts Institute for Research in Inflammatory Bowel Disease, Weill Cornell Medicine, New York, NY

23 <sup>12</sup>OPEN, Odense Patient data Explorative Network, Odense University Hospital/Department of Clinical Research,  
24 University of Southern Denmark, Odense, Denmark

25 <sup>13</sup>Nutrition, Metabolism and Genomics Group, Division of Human Nutrition, Wageningen University, Wageningen,  
26 The Netherlands.

27 <sup>14</sup>Norwich Medical School, University of East Anglia, Norwich, UK.

28 \*These authors contributed equally to this work

29 Address correspondence to: Leif Erik Sander, [leif-erik.sander@charite.de](mailto:leif-erik.sander@charite.de)

30 **Live attenuated vaccines are generally highly efficacious and often superior to inactivated**  
31 **vaccines, yet the underlying mechanisms remain largely unclear. Here we identify innate**  
32 **immune recognition of microbial viability as a potent stimulus for T follicular helper (T<sub>FH</sub>)**  
33 **cell differentiation and vaccine responses. Antigen presenting cells (APC) distinguish viable**  
34 **from dead bacteria through the detection of bacterial RNA via Toll-like receptor (TLR)-8.**  
35 **Live bacteria, bacterial RNA, or synthetic TLR8 agonists induce a specific cytokine profile**  
36 **in human and porcine APC and promote T<sub>FH</sub> cell differentiation, which dead bacteria and**  
37 **other TLR ligands fail to induce. Accordingly, vaccination with live, but not heat killed**  
38 **attenuated bacteria induces T<sub>FH</sub> cell differentiation and robust humoral immune responses**  
39 **in swine. A hypermorphic TLR8 polymorphism was associated with enhanced protective**  
40 **immunity elicited by a live bacterial vaccine against tuberculosis in a human cohort. We**  
41 **provide mechanistic insights into the superiority of live vaccines and we identify TLR8 as a**  
42 **key regulator of T<sub>FH</sub> cell differentiation and a promising target for T<sub>FH</sub>-skewing adjuvants.**

43

44

45 INTRODUCTION

46 Live attenuated microbes represent the first generation of vaccines and have contributed to the  
47 extinction or dramatic reduction of deadly diseases such as smallpox or rabies<sup>1, 2, 3</sup>. Their  
48 unparalleled success was based on empiricism<sup>4</sup>. Yet, their exact mechanisms of action, the  
49 frequently observed superiority over inactivated vaccine preparations<sup>5, 6</sup>, and their exceptional  
50 capacity to induce protective, often lifelong immunity still remain largely unexplained.

51 As the first line of defense, the innate immune system detects microbial invaders and  
52 carefully scales the level of infectious threat in order to elicit appropriate, well-measured immune  
53 responses<sup>7</sup>. We have previously described an inherent capacity of murine innate immune cells to  
54 discriminate live from dead microorganisms<sup>8</sup>. Viable and thus potentially harmful microorganisms  
55 contain specialized pathogen associated molecular patterns (PAMPs) as molecular signatures of  
56 microbial life, which we **termed** *vita*-PAMPs<sup>8</sup>. We identified bacterial messenger RNA as a *vita*-  
57 PAMP, detection of which alerts the innate immune system, **elicits** specific inflammatory immune  
58 responses, **and** promotes humoral immunity in mice<sup>8</sup>. However, the role of *vita*-PAMPs and their  
59 receptors in regulating human immune responses is unknown.

60 Given the importance of innate immune signals in shaping adaptive immune responses<sup>9</sup>,  
61 we asked whether innate immune recognition of bacterial viability affects ensuing T helper cell  
62 responses and particularly the differentiation of T follicular helper (T<sub>FH</sub>) cells. Since their  
63 identification<sup>10, 11</sup>, this subset of CD4<sup>+</sup> T cells has progressively emerged as a pivotal regulator of  
64 the germinal center response and humoral immunity<sup>12, 13, 14</sup>. Differentiation of T<sub>FH</sub> cells constitutes  
65 a complex, multilayered process involving the combination of several molecular and cellular  
66 signals at distinct microanatomical sites<sup>12, 13, 14</sup>. Intense research in recent years has unraveled the  
67 complexity of T<sub>FH</sub> cell development, their transcriptional control<sup>14, 15, 16, 17</sup>, and their molecular  
68 interactions with B cells in the germinal centers, following the initial priming in the T cell zone<sup>18</sup>.  
69 <sup>19, 20, 21</sup>. Far less **is known about** the early stages of T<sub>FH</sub> differentiation and the role of APC-derived  
70 innate immune signals in controlling this process, **especially in humans**. Targeted mobilization of  
71 T<sub>FH</sub> responses poses a major hurdle in vaccine development. Therefore, the identification of  
72 particular innate immune pathways with T<sub>FH</sub>-skewing capacity in humans would be highly  
73 desirable for the rational design of T<sub>FH</sub>-targeted vaccine adjuvants.

74 In this study, we systematically compared human immune responses to live and dead  
75 attenuated bacteria and found that innate immune recognition of bacterial viability leads to  
76 transcriptional remodeling in professional APC, and induces T<sub>FH</sub> promoting signals, most  
77 importantly IL-12. Human APC distinguish precisely between viable and dead bacteria  
78 independently of virulence, through the detection of bacterial RNA via the endosomal RNA sensor  
79 TLR8. Recognition of live bacteria by human APC promotes the differentiation of naïve CD4<sup>+</sup> T  
80 cells into IL-21 producing BCL6<sup>+</sup>CXCR5<sup>+</sup>ICOS<sup>+</sup>PD1<sup>+</sup> T<sub>FH</sub> cells. Activation of TLR8 in APC by  
81 its natural ligand bacterial RNA, or by synthetic agonists promotes subsequent T<sub>FH</sub> cell  
82 differentiation. In contrast, killed bacteria or other TLR agonists, including licensed vaccine  
83 adjuvants, which were tested head-to-head with TLR8 agonists, failed to do so even at high  
84 concentrations. Consequently, TLR8 gene silencing in APC inhibited bacterial-induced T<sub>FH</sub>  
85 programming. Confirming the importance of viability recognition *in vivo*, we observed robust T<sub>FH</sub>  
86 differentiation in swine in response to immunization with a live attenuated strain of *Salmonella*  
87 *enterica* serovar Typhimurium, a commonly used vaccine in pig farming. This is the first  
88 description of T<sub>FH</sub>-like cells in pigs, which were not increased after immunization with the heat  
89 killed version of the same vaccine. Outbred farm pigs represent a valuable immunological model  
90 and they are a major target population for prophylactic vaccines, in order to decrease antibiotic  
91 consumption and the development of antibiotic resistance. Finally, a case-control study revealed a  
92 strong association of a hypermorphic *TLR8* polymorphism and *Bacillus Calmette-Guérin* (BCG)-  
93 induced protection from tuberculosis infection, linking TLR8 function to protective immunity in  
94 response to a live attenuated vaccine in humans. In summary, we identify recognition of bacterial  
95 viability as a conserved innate immune checkpoint that preferentially promotes T<sub>FH</sub> cell  
96 differentiation and humoral immunity. Our study highlights the importance of studying innate  
97 immunity in humans and we propose *vita*-PAMP receptors such as TLR8 as promising targets for  
98 T<sub>FH</sub>-skewing adjuvants to improve the efficacy of modern subunit vaccines.

99

100

## 101 RESULTS

### 102 *Detection of live bacteria promotes T<sub>FH</sub> cell differentiation*

103 In order to assess the contribution of innate immune signals on human T<sub>FH</sub> cell differentiation, we  
104 co-cultured classical human CD14<sup>+</sup>CD16<sup>-</sup> monocytes, as APC, with autologous naïve CD4<sup>+</sup> T  
105 cells. APC were stimulated with either live avirulent thymidine auxotrophic (*thyA*<sup>-</sup>, replication  
106 defective) *Escherichia coli* (hereafter referred to as EC)<sup>8</sup> or a heat killed versions of the same *E.*  
107 *coli* (HKEC). We intentionally chose avirulent auxotrophic bacteria in order to selectively analyze  
108 the impact of bacterial viability without confounding effects due to virulence factors and bacterial  
109 replication<sup>8</sup>. Ninety minutes after bacterial stimulation of APC we added antibiotics and naïve  
110 CD4 T cells and assessed T helper cell differentiation five days later. Notably, stimulation of APC  
111 with live bacteria induced naïve CD4<sup>+</sup> T cells to produce large quantities of T<sub>FH</sub>- and T<sub>H</sub>1-  
112 signature cytokines IL-21 and interferon- $\gamma$  (IFN- $\gamma$ ), respectively (Fig. 1a,b). This response was  
113 virtually absent when APC were stimulated with heat killed bacteria or medium alone (Fig. 1a,b).  
114 In contrast to IL-21 production, T cell proliferation rates were similar in all conditions, and IL-17  
115 was produced at moderate levels regardless of bacterial viability (Fig. 1a,b). In line with the  
116 increased IL-21 production, stimulation with viable but not killed bacteria also promoted the  
117 expression of prototypical T<sub>FH</sub> cell surface markers CXCR5, ICOS and PD-1<sup>10, 11, 22</sup>(Fig. 1c,d and  
118 Supplementary Fig. 1a).

119 B-cell lymphoma-6 (BCL6) is considered the lineage defining transcription factor of T<sub>FH</sub> cells, and  
120 it is required for successful T<sub>FH</sub> cell development<sup>16, 17</sup>. APC stimulated with live bacteria induced  
121 BCL6 and IL-21 co-expression in CD4<sup>+</sup> T cells, whereas APC stimulated with killed bacteria failed  
122 to do so (Fig. 1e,f). The observed effects were not restricted to monocytes, since similar results  
123 were obtained using primary human CD1c<sup>+</sup> myeloid dendritic cells (mDC-1) as APC instead of  
124 monocytes (Fig. 1g,h). Other T helper cell lineage defining transcription factors T-bet (encoded  
125 by TBX21) and GATA-3 were downregulated by bacterial stimulation of APC as compared to T  
126 cells activated with unstimulated APC, whereas ROR $\gamma$ T (encoded by RORC) and MAF were  
127 slightly increased in both EC and HKEC conditions (Fig. 1i, Supplementary Fig. 1b).

### 128 *Functional properties of de novo differentiated T<sub>FH</sub> cells*

129 Differentiation of T<sub>FH</sub> cells occurs in a complex multi-step process<sup>12, 13</sup>. An initial priming step  
130 involving conventional APC<sup>23</sup> induces transient expression of T<sub>FH</sub>-associated genes in a subset of

131 CD4<sup>+</sup> T cells<sup>15</sup> allowing for their migration towards the B cell zone within secondary lymphoid  
132 organs<sup>12, 24</sup>. There, interaction with B cells, which then take over antigen presentation, stabilizes  
133 the T<sub>FH</sub> differentiation program and initiates the germinal center response<sup>12, 14, 25, 26</sup>. In order to  
134 mimic the first two stages of T<sub>FH</sub> cell differentiation we employed a sequential co-culture system,  
135 in which naïve CD4<sup>+</sup> T cells were first primed by EC-stimulated monocytes as in Figure 1, re-  
136 purified from the culture after five days, and subsequently co-cultured with autologous naïve B  
137 cells for an additional seven days. Notably, the T<sub>FH</sub> phenotype was maintained and increased over  
138 the combined culture period of 12 days (**Fig. 2a**) indicating that the initial priming did not merely  
139 induce transiently IL-21-expressing effector cells<sup>27</sup>.

140 In order to assess their functionality as *bona fide* B cell helpers, we sorted *de novo*  
141 differentiated CD4<sup>+</sup>CD45RA<sup>-</sup>CXCR5<sup>+</sup> T<sub>FH</sub> cells and compared them side by side with autologous  
142 naïve CD4<sup>+</sup>CD45RA<sup>+</sup>CXCR5<sup>-</sup> T cells for their ability to promote plasma cell differentiation of co-  
143 cultured B cells. Indeed, CXCR5<sup>+</sup> T<sub>FH</sub> generated in response to live bacteria induced robust  
144 differentiation of CD27<sup>++</sup>CD38<sup>+</sup> plasma cells, which naïve T cells from the same donor failed to  
145 induce (**Fig. 2b,c**). This was also mirrored by the robust IgG production induced by co-culture  
146 with *in vitro* differentiated T<sub>FH</sub> cells, which was not observed with B cells alone or **after** co-culture  
147 with naïve T cells (**Fig. 2d**). CXCR5<sup>-</sup> T cells sorted from the same cultures provided relatively  
148 weaker help compared to CXCR5<sup>+</sup> T cells (**Supplementary Fig. 2a-d**). Collectively, the results  
149 demonstrate that innate immune recognition of viable, but not killed bacteria by human APC elicits  
150 potent differentiation signals for the generation of fully functional T<sub>FH</sub> cells.

### 151 ***Detection of bacterial viability uniquely shapes the cytokine profile of APC***

152 In order to characterize the innate immune signals that control T<sub>FH</sub> programming upon recognition  
153 of bacterial viability, we compared the transcriptional responses of human APC to live and dead  
154 bacteria. In contrast to the drastically altered T cell responses (**Fig. 1**), detection of live and dead  
155 bacteria elicited very similar transcriptional programs in human monocytes (**Fig. 3a**). The highly  
156 congruent response to EC and HKEC reflects the high similarity between the two stimuli, both of  
157 which contain an abundance of PAMPs and lead to strong APC activation through engagement of  
158 a multitude of pattern recognition receptors<sup>8</sup>. Strikingly, a narrow set of 193 genes was  
159 differentially regulated in response to live compared to dead bacteria, including the genes encoding  
160 for inflammatory cytokines TNF (**TNF**) and IL-12p40 (**IL12B**) (**Fig. 3a,b** and **Supplementary**

161 **Table 1**). Accordingly, IL-12 and TNF were released nearly exclusively in response to live but not  
162 dead bacteria, whereas other cytokines including IL-6, IL-10, IL-23, and GM-CSF were produced  
163 regardless of bacterial viability (**Fig. 3c**). Thus, human APC discriminate precisely between live  
164 and dead bacteria and remodel their transcriptional program and subsequent cytokine production  
165 in response to the detection of bacterial viability. Differential expression of IL-12 and TNF was  
166 unexpected given previous observations in murine APC, which produce large amounts of TNF and  
167 IL-12 in response to both live and killed bacteria or purified bacterial cell wall components<sup>8</sup>.  
168 Similar to murine APC<sup>8</sup> though, IL-1 $\beta$  release was specifically induced by viable bacteria in  
169 human APC indicating inflammasome activation (**Fig. 3c**)<sup>8</sup>. Production of TNF and IL-12 was  
170 dependent on the presence of live bacteria and could not be restored by higher doses of killed  
171 bacteria (**Fig. 3d**). Other bacterial species, including avirulent Gram-positive *Bacillus subtilis*, and  
172 BCG, an attenuated strain of *Mycobacterium bovis* and widely-used live vaccine against  
173 tuberculosis (TB), elicited comparable cytokine patterns (**Fig. 3e**), indicating that the response to  
174 bacterial viability is conserved and largely independent of bacterial species-specific features. In  
175 contrast to the distinct cytokine patterns elicited by live and dead bacteria, both stimuli induced a  
176 similar up-regulation of various maturation markers in APC, again emphasizing the intact innate  
177 recognition of both stimuli (**Fig. 3f**).

#### 178 ***'Viability-induced' T<sub>FH</sub> responses are mediated by APC-derived IL-12***

179 Based on these results, we hypothesized that APC-derived cytokines were responsible for the  
180 observed early T<sub>FH</sub> differentiation upon detection of live bacteria. Indeed, polyclonally activated  
181 CD4<sup>+</sup> T cells expressed high levels of IL-21 when differentiated in conditioned culture  
182 supernatants from APC that had been stimulated with live bacteria (**Fig. 4a,b**). Conditioned culture  
183 supernatants from HKEC-treated APC failed to induce substantial IL-21 production by T cells.  
184 Thus, apart from slightly higher background IL-21 and IFN- $\gamma$  levels, the cell contact-free system  
185 essentially reproduced the results of the co-culture experiments, which allow for direct cell contact  
186 between APC and T cells (**Fig. 1**). As in the co-cultures, no differences in proliferation rates and  
187 IL-17 production were observed (**Supplementary Fig. 3a,b**). These results support a dominant  
188 role of APC-derived cytokines in the initial stages of T<sub>FH</sub> differentiation in response to live EC.

189 Various cytokines and cytokine combinations have previously been found to promote T<sub>FH</sub>  
190 cell differentiation in mice, including IL-21 itself, IL-6, IL-27 and type I IFN<sup>28, 29, 30, 31</sup>, whereas

191 IL-12, TGF- $\beta$ , and to a lesser extent IL-23, IL-6, and potentially IL-27, contribute to the  
192 differentiation of human T<sub>FH</sub> cells<sup>30, 32, 33, 34, 35, 36</sup>. Yet it is unclear which cytokines are responsible  
193 for infection- or *vita*-PAMP-induced human T<sub>FH</sub> cell differentiation. We compared cytokine levels  
194 in the EC-stimulated APC supernatants with subsequent IL-21 production by CD4<sup>+</sup> T cells and  
195 found a strong correlation between APC-derived IL-12 levels and subsequent IL-21 production by  
196 activated T cells, whereas TNF and IL-6 levels did not correlate with T cell-derived IL-21 (**Fig.**  
197 **4c**). Neutralization of IL-12 in APC supernatants virtually abolished T<sub>FH</sub> differentiation, without  
198 affecting T cell proliferation rates (**Fig 4d-f** and **Supplementary Fig. 3a**). In contrast,  
199 neutralization of IL-6 and IL-27 had no significant effect, whereas TNF blockade partially  
200 inhibited T<sub>FH</sub> differentiation (**Fig. 4d-f**). Conversely, supplementing control-APC supernatants  
201 with recombinant IL-12 restored T<sub>FH</sub> cell differentiation (**Fig. 4d-f**). Recombinant TNF alone was  
202 insufficient to promote a T<sub>FH</sub> phenotype, indicating that it might play a minor role or act in concert  
203 with IL-12 or other APC-derived factors (**Fig. 4g**). Recognition of *vita*-PAMPs by APC induces  
204 robust production of IL-1 $\beta$  (**Fig. 3c**) and type I IFN<sup>8</sup> in mice. Human T<sub>FH</sub> cell differentiation was  
205 only partially diminished by neutralization of IL-1 $\beta$  and supplementation of control supernatants  
206 with recombinant IL-1 $\beta$  alone was insufficient to support T<sub>FH</sub> cell differentiation (**Supplementary**  
207 **Fig.3d-f**), indicating that IL-1 $\beta$  may have additive effects in humans, consistent with previous  
208 observations<sup>32</sup>. Blocking IFN- $\beta$  or supplementing recombinant IFN- $\beta$  did not alter human T<sub>FH</sub> cell  
209 differentiation in our experiments (**Supplementary Fig.3d-f**). While additional membrane bound  
210 mediators such as ICOSL<sup>20</sup> and OX40L<sup>37</sup> contribute to different stages of T<sub>FH</sub> differentiation *in*  
211 *vivo*, we found no major differences in the surface levels of both molecules on APC after  
212 stimulation with live and dead bacteria (**Fig. 3f**). Although this does not exclude an important role  
213 for these membrane-bound molecules at later stages, we conclude that IL-12 is the critical innate  
214 immune signal produced in response to live bacteria to instruct early T<sub>FH</sub> cell priming in humans.

### 215 *Human APC sense bacterial viability via TLR8*

216 Vaccine adjuvants activate the innate immune system and as such they are essential components  
217 of all clinically relevant subunit vaccines<sup>38</sup>. Targeted activation of T<sub>FH</sub>-polarizing innate immune  
218 pathways would be highly desirable for vaccination purposes, given the broad protection offered  
219 by high titers of neutralizing and opsonizing antibodies. We therefore investigated the nature of  
220 the innate immune receptor(s) and their ligands that elicit ‘viability-induced’ T<sub>FH</sub> differentiation



221 signals in APC. Assuming a critical role for *vita*-PAMPs<sup>8</sup>, we supplemented HKEC with various  
222 PAMPs and compared subsequent cytokine responses. Only ligands of the endosomal ssRNA  
223 receptors TLR7/8 restored IL-12 and TNF production to levels comparable with viable bacteria  
224 (**Fig. 5a**). Inhibition of actin polymerization and phagocytosis using Cytochalasin D as well as  
225 blockade of endolysosomal acidification with Bafilomycin A abrogated EC-induced production of  
226 IL-12 but not IL-6, further suggesting an involvement of endosomal TLRs in the sensing of viable  
227 bacteria (**Supplementary Fig. 4a**).

228 Since human monocytes express TLR8 but only low levels of TLR7 (**Supplementary Fig.**  
229 **4b**)<sup>39</sup>, and TLR8 has been recently shown to recognize bacterial RNA<sup>40, 41</sup>, we reasoned that TLR8  
230 might be the primary human *vita*-PAMP receptor for live bacteria. Indeed, endosomal delivery of  
231 bacterial RNA fully restored cytokine production to levels comparable to those induced by live  
232 bacteria and synthetic TLR7/8 agonists (**Fig 5b**) and induced upregulation of activation markers  
233 on APC (**Supplementary Fig. 4c**). Conversely, silencing the expression of TLR8 and its essential  
234 signaling adaptor molecule MyD88 by RNA interference abrogated IL-12p70 and TNF release in  
235 response to viable EC (**Fig. 5c,d**). Production of IL-6, which does not require bacterial viability,  
236 was not affected by TLR8- or MyD88 gene silencing (**Fig. 5c,d**).

237 These results identify TLR8 as the primary sensor for bacterial viability and critical regulator of  
238 cytokine responses, including IL-12 production in human APC.

### 239 *Detection of bacterial RNA via TLR8 induces T<sub>FH</sub> differentiation*

240 In line with its critical role in the recognition of live bacteria by human APC, TLR8 ligation dose-  
241 dependently induced T<sub>FH</sub> cell differentiation (**Fig. 6a-c**). In contrast, all other TLR ligands tested,  
242 including the licensed vaccine adjuvants monophosphoryl lipid A (TLR4 agonist) and CpG-DNA  
243 (TLR9 agonist), failed to promote T<sub>FH</sub> cell responses even at high concentrations (**Fig. 6a-c**).  
244 Similar to live bacteria, TLR8 activation by purified bacterial RNA resulted in high levels of T<sub>FH</sub>  
245 cells and IL-21 production (**Fig. 6d, e**), demonstrating that innate immune recognition of bacterial  
246 RNA is a potent stimulator of T<sub>FH</sub> differentiation signals. Finally, silencing TLR8 expression in  
247 APC diminished their capacity to promote T<sub>FH</sub> differentiation in response to live bacteria (**Fig. 6f,**  
248 **g**). Collectively, these results identify TLR8 as the critical sensor for bacterial viability in human  
249 APC and critical inducer of subsequent T<sub>FH</sub> responses.

250

251 ***Recognition of bacterial viability is conserved in porcine APC***

252 Domestic pigs (*Sus scrofa domestica*) are increasingly utilized for biomedical and pharmaceutical  
253 studies due to the substantial analogies between porcine and human physiology<sup>42, 43</sup>. The porcine  
254 and the human immune system also shares many similarities<sup>43</sup>, including expression and function  
255 of TLR8<sup>44</sup>. Owing to the drastic increase in antibiotic resistance rates and frequent emergence of  
256 veterinary pathogens in industrial animal farming, there is a growing need for prophylactic  
257 vaccines in pigs, making them both an attractive model and a relevant target population for vaccine  
258 studies. Here we assessed the relevance of viability recognition for T<sub>FH</sub> differentiation and vaccine  
259 responses in pigs.

260 Porcine monocytes (CD172<sup>+</sup>CD14<sup>+</sup>) and dendritic cells (DC, CD172<sup>+</sup>CD14<sup>-</sup>) were sorted from  
261 spleen samples of domestic pigs and stimulated with live and dead bacteria. We used **the** thymidine  
262 auxotrophic *E. coli* (EC) and an attenuated strain of *Salmonella enterica* serovar Typhimurium  
263 (ST) distributed under the trade name of Salmoporc-STM as a live *Salmonella* vaccine for pigs<sup>45</sup>.  
264 Salmoporc-STM are histidine- and thymidine auxotrophs leading to severe growth attenuation in  
265 the absence of exogenous histidine and thymidine. Similar to human APC, porcine monocytes  
266 and DC secreted high levels of IL-12 in response to live bacteria and TLR8 agonist CL075, but  
267 not upon stimulation with heat killed ST (HKST) and HKEC (**Fig. 7a,b**). Secretion of IL-6 was  
268 similarly induced by live and dead bacteria (**Fig. 7a, b**). **Selective induction of IL-12 by live**  
269 **bacteria was consistently observed, yet statistical testing did not reveal significant differences**  
270 **due to high inter-experimental variation in cytokine production. Purified bacterial RNA also**  
271 **promoted increased secretion of IL-12p40 in porcine monocytes, not observed with ligands of**  
272 **TLR2 and TLR4 (Supplementary Fig. 5).** In order to confirm that the mechanisms of ‘viability  
273 recognition’ are conserved between human and porcine APC, we silenced the expression of TLR8  
274 in porcine CD14<sup>+</sup> monocytes by RNAi. Knock down of TLR8 abrogated IL-12p40 expression in  
275 response to live ST, whereas IL-6 production, which is induced independently of bacterial  
276 viability, was **un**affected by TLR8 **silencing** (**Fig. 7c**). Hence, recognition of bacterial viability  
277 requires TLR8 in human and porcine APC. We next assessed the impact of bacterial viability on  
278 porcine T<sub>FH</sub> cell differentiation. **S**plenocytes (containing APCs and CD4<sup>+</sup> T cells) were stimulated  
279 with increasing doses of live ST or HKST for one hour, followed by addition of antibiotics to  
280 prevent residual bacterial growth. Concanavalin A (ConA) was **used** to induce polyclonal T cell  
281 proliferation. We observed a dose-dependent increase in the frequency of CD4<sup>+</sup>IL-21<sup>+</sup> **BCL6**<sup>+</sup>

282 T<sub>FH</sub>-like cells in response to ST, which was absent upon stimulation with HKST, regardless of the  
283 bacterial dose (**Fig. 7d,e**). Hence, innate recognition of bacterial viability, i.e. *vita*-PAMPs,  
284 specifically controls porcine T<sub>FH</sub> differentiation. These findings represent the first demonstration  
285 of T<sub>FH</sub>-like cells in swine. When we compared the capacity of soluble PAMPs to induce a T<sub>FH</sub>  
286 phenotype in splenocyte cultures, we found that TLR8 agonists bacterial RNA and CL075, but not  
287 TLR4 agonist LPS induced CD4<sup>+</sup>IL21<sup>+</sup> BCL6<sup>+</sup> T cells (**Fig. 7f**). Thus, recognition of bacterial  
288 viability via TLR8 plays a critical role for porcine T<sub>FH</sub> cell differentiation.

### 289 *Bacterial viability promotes T<sub>FH</sub> differentiation in vivo*

290 To directly assess the role of innate immune detection of bacterial viability for T<sub>FH</sub> cell responses  
291 *in vivo*, we vaccinated domestic pigs with live attenuated ST (Salmoporc-STM), or with an  
292 equivalent dose of heat inactivated vaccine (HKST), or solvent as control. Increased frequencies  
293 of CD4<sup>+</sup>IL-21<sup>+</sup> BCL6<sup>+</sup> T<sub>FH</sub>-like cells were detected in the draining (dorsal superficial cervical)  
294 lymph node and in the spleen of animals immunized with the live attenuated vaccine compared to  
295 animals receiving the heat killed vaccine or saline control (**Fig. 8a, b**). The specific effects of the  
296 live vaccine on T<sub>FH</sub> differentiation was underscored by the fact that other markers of T effector  
297 cell differentiation, including lineage defining transcription factors Tbet (T<sub>H1</sub>) and FoxP3 (T<sub>REG</sub>)  
298 were similarly altered in T cells from the ST and the HKST vaccine group (**Supplementary Fig**  
299 **6a-d**).

300 As a further indication of enhanced follicular helper cell responses following ST vaccination, we  
301 observed markedly increased PAX5<sup>+</sup> B cell follicles in the spleen of ST vaccinated pigs compared  
302 to controls, which was not observed in the HKST group when compared to controls (**Fig. 8c, d**),  
303 albeit no statistical difference was detected between the ST and the HKST group. B cell follicles  
304 were highly enriched in KI67<sup>+</sup>PAX5<sup>+</sup> B cells, indicative of active germinal centers (**Fig. 8e**,  
305 **Supplementary Fig. 7a**), but were negative for BCL2 ruling out malignant transformation  
306 (**Supplementary Fig. 7b**). We also found increased CD3<sup>-</sup>CD8<sup>-</sup>SLAII<sup>+</sup>IgM<sup>+</sup>CD2<sup>+/-</sup>CD21<sup>-</sup> antibody  
307 forming cells (AFC) / plasma cells (PC)<sup>46</sup> in ST- as compared to HKST-vaccinated animals (**Fig.**  
308 **8f**). Importantly, higher levels of *Salmonella*-binding serum-IgG were detected after vaccination  
309 with live ST, as a direct evidence of enhanced humoral immunity in response to the live, compared  
310 to the killed vaccine (**Fig. 8g**).

311 These results corroborated our findings with primary human cells, and they establish the  
312 recognition of bacterial viability as an essential driver of vaccine-induced T<sub>FH</sub> cell responses *in*  
313 *vivo*.

#### 314 ***A functional TLR8 polymorphism is associated with vaccine protection in humans***

315 Several functional polymorphisms in the gene encoding for TLR8 in humans have been  
316 described<sup>47, 48</sup>. The *TLR8* single nucleotide polymorphism (SNP) TLR8-A1G (rs3764880,  
317 hereafter referred to as TLR8-G) alters the start ATG codon into a GTG triplet<sup>47</sup> shifting the signal  
318 peptide by three amino acids with a second in frame ATG (M4) being used as alternative start  
319 codon. We performed *in silico* modeling predictions, based on the published crystal structure of  
320 TLR8<sup>49</sup>. According to these models, the amino acid truncation leads to significant structural  
321 alterations of the protein (**Supplementary Figure 8-10 and Supplementary Text**). Increased  
322 disorder, free energy, and increased flexibility of TLR8-G likely make the receptor better adapted  
323 to side chain rearrangement and dimerization. The larger volume of clefts and cavities on the  
324 surface of TLR8-G, compared to TLR8-A, may increase its potential for ligand binding, whereas  
325 functional pockets and nests are slightly decreased (**Supplementary Fig. 9, 10**). These models  
326 suggest an altered receptor functionality, which may cause a gain-of-function in the TLR8-G  
327 variant. In line with these predictions, APC from individuals carrying either the TLR8-A or TLR8-  
328 G variant showed a slightly enhanced IL-12 response to TLR8 stimulation, but not in response to  
329 TLR4 agonist LPS (**Supplementary Fig. 11a, b**). High inter-donor variation combined with the  
330 moderate gain of function phenotype account for the modest, but significant impact on cytokine  
331 production. Analysis of TLR8-G and TLR8-A function in a standardized reporter cell system  
332 confirmed the gain-of-function phenotype, since reporter cells expressing the TLR8-G variant  
333 showed stronger NF- $\kappa$ B activation in response to TLR8 ligands compared to TLR8-A expressing  
334 cells (**Supplementary Fig. 11c**).

335 Previous studies have associated TLR8-G allele carriage with slower progression of HIV-  
336 infection<sup>47</sup>, and protection against pulmonary TB (PTB)<sup>50</sup>. Here, we assessed TLR8-G allele  
337 distribution in 293 patients with confirmed TB and 165 of their healthy household contacts  
338 (**Supplementary Table 2**). Significantly more controls (53.9%) were homo- or hemizygous  
339 TLR8-G carriers than TB patients (41.3%) (**Fig. 9a, left panel and Supplementary Table 3**). The  
340 TLR8-A allele was associated with significantly increased odds for TB infection (OR=1.94 [1.194-

341 3.156]; $p=0.007$ ), and similar results were found in the PTB subgroup (**Fig. 9a, right panel** and  
342 **Supplementary Table 3**), confirming the protective effect of the TLR8-G allele against PTB as  
343 previously reported<sup>50</sup>. However, further subgroup analyses revealed that TLR8 allele distribution  
344 was in fact significantly different only in subjects who had previously received the BCG vaccine  
345 against TB ( $p=0.002$ ), whereas allele distribution was not different ( $p=0.754$ ) in unvaccinated  
346 subjects (**Fig. 9b** and **Supplementary Table 4**). Consequently, in this study population, BCG-  
347 vaccination is associated with a significant risk protection in TLR8-G carriers (OR=0.280 [CI95%  
348 0.105-0.742]), but not in TLR8-A allele carriers (**Fig. 9c** and **Supplementary Table 4**). These  
349 epidemiological results indicate that TLR8-G carriage is associated with an improved BCG-  
350 vaccine mediated protection without affecting susceptibility to PTB *per se*. The study links TLR8  
351 function to protective immunity in response to a live bacterial vaccine in a large human cohort.

352

## 353 DISCUSSION

354 Our study identifies innate immune recognition of microbial viability as a hard-wired, conserved  
355 immune checkpoint, which critically regulates innate and adaptive immunity. We describe TLR8  
356 as the first *vita*-PAMP receptor in humans and pigs, activation of which renders APC highly  
357 effective **inducers** of T<sub>FH</sub> responses. We provide experimental and epidemiological evidence to  
358 support a critical function of viability recognition and TLR8 in the immune responses to live  
359 attenuated vaccines in humans and pigs.

360 Recent studies in non-human primates have revealed a unique adjuvant activity of TLR8  
361 agonists<sup>51, 52, 53</sup>. Innate immune responses to TLR8 agonist-containing nanoparticles **were highly**  
362 **similar to** responses **evoked by** live BCG, **but** distinct from those **elicited** by various inanimate  
363 vaccines<sup>51</sup>. Supplementation of the commercial alum-adjuvanted pneumococcal glycoconjugate  
364 vaccine (PCV13) with an TLR8 agonist strongly increased IgG responses in newborn rhesus  
365 macaques<sup>52</sup>. We show that live attenuated bacteria as well as purified bacterial RNA or synthetic  
366 TLR8 agonists selectively modulate the cytokine profile of APC and promote T<sub>FH</sub> responses,  
367 which dead bacteria and other TLR ligands fail to induce. Moreover, we found a functional TLR8  
368 polymorphism to be associated with increased cytokine production in response to TLR8 synthetic  
369 ligands and with enhanced protection afforded by BCG vaccination in early life, clearly supporting  
370 a link between TLR8 functionality and vaccine responses in humans (**Fig. 9**). These findings may

371 also help to explain the diverging efficacies of BCG-vaccination reported in various studies<sup>54</sup>.  
372 **While the** role of T<sub>FH</sub> cells **cannot** be assessed in this retrospective case-control study, mounting  
373 evidence suggest a critical contribution of T<sub>FH</sub> and a T cell-dependent antibody responses in BCG  
374 vaccination and anti-mycobacterial immunity<sup>55, 56, 57, 58</sup>. In particular, IL-12 has been recently  
375 linked to the development of T<sub>FH</sub>-like cells at the site of TB infection<sup>58</sup>. **Supporting** the notion that  
376 BCG vaccination elicits T<sub>FH</sub> cell dependent responses, we found increased T<sub>FH</sub> cell frequencies in  
377 the spleens of pigs 30 days after BCG vaccination (**Supplementary Fig. 12**). **Although** commonly  
378 used live vaccines are diverse and likely activate multiple pathways<sup>59</sup>, we propose innate immune  
379 recognition of microbial viability and subsequent **promotion** of T cell-driven immunity as a  
380 unifying motif in the responses to live attenuated vaccines.

381 In order to further validate our findings, we studied vaccine responses to live attenuated  
382 bacteria in pigs. Vaccine studies in large animals such as pigs are challenging, due to obvious  
383 limitations in group size and a relative lack of advanced tools and experimental models (e.g. TCR-  
384 transgenic or PRR-deficient animals) compared to mice. On the other hand, domestic pigs offer  
385 major advantages over established rodent models, given their closer resemblance of human  
386 physiology with regards to size, life span, organ anatomy, diet, circadian rhythm, and immunity<sup>42</sup>.  
387 <sup>60</sup>. **Conventional non**-specific-pathogen-free(SPF) housing and outbreeding of the animals also  
388 makes for a better comparability to humans. More importantly, besides serving as a model,  
389 domestic farm animals represent a critical target population for vaccination in order to improve  
390 animal- and public health. High antibiotic consumption in industrial animal farming is considered  
391 a major driving force of antibiotic resistance<sup>61</sup>, and efficacious veterinary vaccines are therefore  
392 urgently needed<sup>62</sup>. Here we used a well-established swine vaccine against *Salmonella enterica*  
393 infections to dissect the immune responses to live attenuated bacteria in pigs. Our study provides  
394 the first evidence of T<sub>FH</sub>-like cells in pigs and describes their induction upon recognition of  
395 bacterial viability *in vitro* and *in vivo* (**Fig. 7 and 8**). While future studies are clearly needed to  
396 fully characterize the generation of protective immunity in pigs, our study contributes new insights  
397 into the mechanisms of actions of live attenuated vaccines and highlights swine as a valuable  
398 species for vaccine and T<sub>FH</sub> cell research.

399 In contrast to the detailed knowledge **of** the transcriptional regulation of T<sub>FH</sub> cells and their  
400 interaction with B cells, few studies have investigated the T<sub>FH</sub>-polarizing potential of different  
401 innate immune stimuli like vaccine adjuvants. The requirement for conventional APC in priming

402 T<sub>FH</sub> cell responses is evident<sup>12, 14, 23</sup> and it was previously suggested that innate activation signals  
403 could determine the capacity of APC to prime T<sub>FH</sub> cell responses. Yet, the nature of T<sub>FH</sub>-favoring  
404 innate immune stimuli has remained largely unknown. Several studies have addressed the impact  
405 of TLR activation on the development of T<sub>FH</sub> cells and germinal center formation in mice<sup>63, 64, 65,</sup>  
406 <sup>66, 67, 68, 69</sup>. For instance, it has been reported that monocyte-derived dendritic cells (Mo-DC) are  
407 important stimulators of T<sub>FH</sub> cell responses in mice, especially when activated via TLR9<sup>70</sup>.  
408 However, T<sub>FH</sub> cell differentiation in mice and humans differs substantially, with regards to the  
409 involved cytokines, as well as the innate immune receptor repertoires in mice and human APC.  
410 This is exemplified by the differential functionality of human and murine TLR8, the latter being  
411 irresponsive to ssRNA<sup>71</sup>. These factors severely hamper the translation of findings from studies in  
412 laboratory mice to human T<sub>FH</sub> cell- and vaccine responses<sup>71</sup>. Human monocytes **hardly induce** T<sub>FH</sub>  
413 differentiation in response to CpG DNA compared to stimulation with viable bacteria and TLR8  
414 agonists (**Fig. 6a-c**). Previous work **suggested** that heat killed bacteria and bacterial  
415 lipopolysaccharide (LPS) were sufficient to induce T<sub>FH</sub> cell differentiation by human *in vitro*  
416 differentiated Mo-DC<sup>35</sup>. However, Mo-DC produce large quantities of bioactive IL-12, due to the  
417 enhancing effects of IL-4 contained in the differentiation medium<sup>72</sup>. In contrast, primary  
418 CD14<sup>+</sup>CD16<sup>-</sup> monocytes, as well as porcine monocytes and DC, secrete high amounts of IL-12 in  
419 response to live bacteria and TLR8 ligation, while production of IL-12 and the T<sub>FH</sub>-skewing  
420 capacity is not observed when APC are stimulated with heat killed bacteria or LPS (**Fig. 3, Fig.**  
421 **6a, b, Fig. 7a and Supplementary Fig. 5**). Moreover, we detected an increase in CD4<sup>+</sup>IL-21<sup>+</sup>  
422 **BCL6**<sup>+</sup> T cells following *ex vivo* culture of **porcine** splenocytes with increasing doses of ST, which  
423 was not observed with HKST (**Fig. 7d-e**). Similarly, CD4<sup>+</sup>IL-21<sup>+</sup> **BCL6**<sup>+</sup> T cells increased in the  
424 draining lymph nodes and in the spleens of pigs following vaccination with a live attenuated  
425 *Salmonella* strain, which was not observed upon immunization with the killed version of the same  
426 bacterium (**Fig. 8a, b**). The latter contains large quantities of PAMPs, including LPS, yet it did not  
427 induce T<sub>FH</sub> cell differentiation, further underscoring the dependency of T<sub>FH</sub> cell responses on  
428 bacterial viability and *vita*-PAMPs.

429 **So far, primary immunodeficiencies (PID) associated with TLR8 deficiency have not been**  
430 **reported. However, patients with gene defects in TLR adaptor proteins MyD88 or IRAK-4 suffer**  
431 **from PID and show a higher susceptibility to bacterial infection<sup>73, 74</sup>. The frequency of T<sub>FH</sub> cells**  
432 **has not been investigated in individuals with these rare gene defects.**

433 Individuals harbouring loss of function mutations in the IL-12 receptor (IL12R1B), the  
434 cytokine driving T<sub>FH</sub> cell differentiation in response to TLR8 ligation, display lower numbers of  
435 circulating T<sub>FH</sub> cells and reduced GC formation in lymph nodes<sup>34</sup>. Other studies have reported a  
436 less pronounced phenotype in older adults, however these studies investigated fewer individuals<sup>75</sup>.  
437 <sup>76</sup>. Naïve CD4<sup>+</sup> T cells isolated from *IL12R1B* deficient individuals fail to induce IL-21 in response  
438 to IL-12 stimulation *in vitro*<sup>75</sup>. A similar phenotype was observed with T cells from individuals  
439 harbouring a heterozygous *STAT3* deficiency<sup>75</sup>, which also exhibit reduced circulating T<sub>FH</sub> cells<sup>75</sup>.  
440 <sup>76</sup>. Notably, antibody levels are largely normal in *IL12R1B*-deficient individuals, yet serum IgG  
441 against tetanus toxoid have a lower avidity, which was not observed with viral antigens, possibly  
442 due to longer persistence of the antigen<sup>34</sup>. These observations highlight our need to better  
443 characterize human immune responses in PID patients, which will allow the identification of non-  
444 redundant signaling modules, as well as potential compensation mechanisms.

445 Given the broad functionality of high affinity antibody responses, it has been proposed that  
446 any microbial stimulus or PAMP is likely to induce T<sub>FH</sub> differentiation<sup>12</sup>. Here we challenge this  
447 wide-spread notion showing that only viable bacteria and agonists of TLR8 promote robust T<sub>FH</sub>  
448 cell formation (**Fig. 6, 7, 8**) and thus provide insights into the proximal innate sensing events that  
449 govern early T<sub>FH</sub> differentiation.

450 High affinity antibodies are indeed a versatile mechanism of defense against many  
451 pathogens, yet uncontrolled T<sub>FH</sub> activation can cause autoimmunity and debilitating diseases<sup>22, 77</sup>.  
452 We have previously proposed that antimicrobial immune responses are tightly scaled to the level  
453 of the microbial threat and we suggested a series of innate immune checkpoints that facilitate an  
454 accurate immunological risk assessment<sup>7</sup>. Here we show that the recognition of bacterial RNA, as  
455 a molecular signature of microbial viability (*vita*-PAMP)<sup>8</sup>, constitutes a critical trigger of T<sub>FH</sub>  
456 differentiation. We propose that the nature and **the** composition of microbial stimuli, i.e. the  
457 presence of *vita*-PAMPs (together with immunogenic antigens), is critical to instruct T<sub>FH</sub> cell  
458 responses. This provides an efficient checkpoint without limiting the versatility of T<sub>FH</sub> cells in **the**  
459 defense against **microbial threats**.

460 The identification of TLR8 as a critical sensor of *vita*-PAMPs and regulator of preferential  
461 T<sub>FH</sub> differentiation provides opportunities for the development of T<sub>FH</sub>-targeted vaccine adjuvants,



462 which are sorely needed to improve existing and future inanimate subunit vaccines against a broad  
463 range of infectious and non-infectious diseases.

464

465 **Acknowledgments:**

466 We thank Désirée Kunkel, Sarah Warth and and Angela Linke for excellent technical assistance.

467 We are indebted to the flow cytometry facility of the Berlin Brandenburg Center for Regenerative  
468 Therapies (BCRT) of the Charité Berlin. We thank Dr. Sven Springer and IDT Biologika GmbH,  
469 for assistance in designing the animal studies and for kindly providing the Salmoporc STM  
470 vaccine. We are thankful to Dr. Riccardo Nifosí of NEST CNR-NANO, Pisa, Italy for his critical  
471 review of the modelling analysis of TLR8.

472 This study was supported by the German Research Council (DFG grant SA1940-2/1 and SFB-  
473 TR84 TP C8 to L.E.S., SFB-TR84 TP B1 to N.S., SFB-TR-84 TP A1/A5 to B.O., SFB-TR84 TP  
474 Z1b to A.D.G. and the DFG-GRK 1673 project to R.R.S.), the European Research Council and the  
475 German Ministry of Science and Education (FP-7 ERA-NET / Infect-ERA consortium  
476 “HaploINFECT” to L.E.S.), the European Society of Clinical Microbiology and Infectious  
477 Diseases (ESCMID research grant to L.E.S.), the Jürgen Manchot Foundation (Doctoral Research  
478 Fellowship to P.G., E.T.H. and S.V.), the Netherlands Nutrigenomics Center, Wageningen  
479 University, The Netherlands (to M.M. and M.B.), the National Institute of Diabetes and Digestive  
480 and Kidney Diseases (DK072201 to J.M.B.), the National Institute of Allergy and Infectious  
481 Diseases (AI073899, AI7570293, AI095245 to J.M.B.), the Fritz Thyssen Foundation (research  
482 grant to A.H.), The Danish National Research Foundation (grant no. DNRF108) to Research  
483 Centre for Vitamins and Vaccines (CVIVA) supporting K.J.J., and The Novo Nordisk Foundation  
484 supporting the pig vaccination experiments at Technical University of Denmark, Federal Ministry  
485 of Education and Research (VIP+ VALNEMCYS project to S.H.).

486 The gene array data will be made publicly available in the public Gene Expression Omnibus  
487 database (GEO, GSE68255).

488

489

490 **References**

- 491 1. Barquet, N. & Domingo, P. Smallpox: the triumph over the most terrible of the ministers of  
492 death. *Ann Intern Med* **127**, 635-642 (1997).  
493
- 494 2. Plotkin, S.A. & Plotkin, S.L. The development of vaccines: how the past led to the future. *Nat*  
495 *Rev Microbiol* **9**, 889-893 (2011).  
496
- 497 3. Minor, P.D. Live attenuated vaccines: Historical successes and current challenges. *Virology* **479-**  
498 **480**, 379-392 (2015).  
499
- 500 4. De Gregorio, E. & Rappuoli, R. From empiricism to rational design: a personal perspective of the  
501 evolution of vaccine development. *Nat Rev Immunol* **14**, 505-514 (2014).  
502
- 503 5. Sridhar, S., Brokstad, K.A. & Cox, R.J. Influenza Vaccination Strategies: Comparing Inactivated  
504 and Live Attenuated Influenza Vaccines. *Vaccines (Basel)* **3**, 373-389 (2015).  
505
- 506 6. Rauh, L.W. & Schmidt, R. Measles Immunization with Killed Virus Vaccine. Serum Antibody  
507 Titers and Experience with Exposure to Measles Epidemic. *Am J Dis Child* **109**, 232-237 (1965).  
508
- 509 7. Blander, J.M. & Sander, L.E. Beyond pattern recognition: five immune checkpoints for scaling  
510 the microbial threat. *Nature Reviews Immunology* **12**, 215-225 (2012).  
511
- 512 8. Sander, L.E. *et al.* Detection of prokaryotic mRNA signifies microbial viability and promotes  
513 immunity. *Nature* **474**, 385-389 (2011).  
514
- 515 9. Iwasaki, A. & Medzhitov, R. Control of adaptive immunity by the innate immune system. *Nat*  
516 *Immunol* **16**, 343-353 (2015).  
517
- 518 10. Breitfeld, D. *et al.* Follicular B helper T cells express CXC chemokine receptor 5, localize to B  
519 cell follicles, and support immunoglobulin production. *J Exp Med* **192**, 1545-1552 (2000).  
520
- 521 11. Schaerli, P. *et al.* CXC chemokine receptor 5 expression defines follicular homing T cells with B  
522 cell helper function. *J Exp Med* **192**, 1553-1562 (2000).  
523
- 524 12. Crotty, S. T follicular helper cell differentiation, function, and roles in disease. *Immunity* **41**, 529-  
525 542 (2014).  
526
- 527 13. Ma, C.S., Deenick, E.K., Batten, M. & Tangye, S.G. The origins, function, and regulation of T  
528 follicular helper cells. *J Exp Med* **209**, 1241-1253 (2012).  
529
- 530 14. Vinuesa, C.G., Linterman, M.A., Yu, D. & MacLennan, I.C. Follicular Helper T Cells. *Annu Rev*  
531 *Immunol* **34**, 335-368 (2016).  
532
- 533 15. Hatzi, K. *et al.* BCL6 orchestrates Tfh cell differentiation via multiple distinct mechanisms. *J Exp*  
534 *Med* **212**, 539-553 (2015).  
535
- 536 16. Johnston, R.J. *et al.* Bcl6 and Blimp-1 are reciprocal and antagonistic regulators of T follicular  
537 helper cell differentiation. *Science* **325**, 1006-1010 (2009).  
538

- 539 17. Nurieva, R.I. *et al.* Bcl6 mediates the development of T follicular helper cells. *Science* **325**, 1001-  
540 1005 (2009).  
541
- 542 18. Cannons, J.L. *et al.* Optimal germinal center responses require a multistage T cell:B cell adhesion  
543 process involving integrins, SLAM-associated protein, and CD84. *Immunity* **32**, 253-265 (2010).  
544
- 545 19. Linterman, M.A. *et al.* IL-21 acts directly on B cells to regulate Bcl-6 expression and germinal  
546 center responses. *J Exp Med* **207**, 353-363 (2010).  
547
- 548 20. Weber, J.P. *et al.* ICOS maintains the T follicular helper cell phenotype by down-regulating  
549 Kruppel-like factor 2. *J Exp Med* **212**, 217-233 (2015).  
550
- 551 21. Good-Jacobson, K.L. *et al.* PD-1 regulates germinal center B cell survival and the formation and  
552 affinity of long-lived plasma cells. *Nat Immunol* **11**, 535-542 (2010).  
553
- 554 22. Ueno, H., Banchereau, J. & Vinuesa, C.G. Pathophysiology of T follicular helper cells in humans  
555 and mice. *Nat Immunol* **16**, 142-152 (2015).  
556
- 557 23. Goenka, R. *et al.* Cutting edge: dendritic cell-restricted antigen presentation initiates the follicular  
558 helper T cell program but cannot complete ultimate effector differentiation. *J Immunol* **187**, 1091-  
559 1095 (2011).  
560
- 561 24. Moser, B., Schaerli, P. & Loetscher, P. CXCR5(+) T cells: follicular homing takes center stage in  
562 T-helper-cell responses. *Trends Immunol* **23**, 250-254 (2002).  
563
- 564 25. Ebert, L.M., Horn, M.P., Lang, A.B. & Moser, B. B cells alter the phenotype and function of  
565 follicular-homing CXCR5+ T cells. *Eur J Immunol* **34**, 3562-3571 (2004).  
566
- 567 26. Kerfoot, S.M. *et al.* Germinal center B cell and T follicular helper cell development initiates in  
568 the interfollicular zone. *Immunity* **34**, 947-960 (2011).  
569
- 570 27. Nakayamada, S. *et al.* Early Th1 cell differentiation is marked by a Tfh cell-like transition.  
571 *Immunity* **35**, 919-931 (2011).  
572
- 573 28. Vogelzang, A. *et al.* A fundamental role for interleukin-21 in the generation of T follicular helper  
574 cells. *Immunity* **29**, 127-137 (2008).  
575
- 576 29. Eddahri, F. *et al.* Interleukin-6/STAT3 signaling regulates the ability of naive T cells to acquire  
577 B-cell help capacities. *Blood* **113**, 2426-2433 (2009).  
578
- 579 30. Batten, M. *et al.* IL-27 supports germinal center function by enhancing IL-21 production and the  
580 function of T follicular helper cells. *J Exp Med* **207**, 2895-2906 (2010).  
581
- 582 31. Cucak, H., Yrlid, U., Reizis, B., Kalinke, U. & Johansson-Lindbom, B. Type I interferon  
583 signaling in dendritic cells stimulates the development of lymph-node-resident T follicular helper  
584 cells. *Immunity* **31**, 491-501 (2009).  
585
- 586 32. Schmitt, N. *et al.* The cytokine TGF-beta co-opts signaling via STAT3-STAT4 to promote the  
587 differentiation of human TFH cells. *Nat Immunol* **15**, 856-865 (2014).  
588

- 589 33. Ma, C.S. *et al.* Early commitment of naive human CD4(+) T cells to the T follicular helper  
590 (T(FH)) cell lineage is induced by IL-12. *Immunol Cell Biol* **87**, 590-600 (2009).  
591
- 592 34. Schmitt, N. *et al.* IL-12 receptor beta1 deficiency alters in vivo T follicular helper cell response in  
593 humans. *Blood* **121**, 3375-3385 (2013).  
594
- 595 35. Schmitt, N. *et al.* Human dendritic cells induce the differentiation of interleukin-21-producing T  
596 follicular helper-like cells through interleukin-12. *Immunity* **31**, 158-169 (2009).  
597
- 598 36. Diehl, S.A., Schmidlin, H., Nagasawa, M., Blom, B. & Spits, H. IL-6 triggers IL-21 production  
599 by human CD4+ T cells to drive STAT3-dependent plasma cell differentiation in B cells.  
600 *Immunol Cell Biol* **90**, 802-811 (2012).  
601
- 602 37. Jacquemin, C. *et al.* OX40 Ligand Contributes to Human Lupus Pathogenesis by Promoting T  
603 Follicular Helper Response. *Immunity* **42**, 1159-1170 (2015).  
604
- 605 38. Coffman, R.L., Sher, A. & Seder, R.A. Vaccine adjuvants: putting innate immunity to work.  
606 *Immunity* **33**, 492-503 (2010).  
607
- 608 39. Hornung, V. *et al.* Quantitative expression of toll-like receptor 1-10 mRNA in cellular subsets of  
609 human peripheral blood mononuclear cells and sensitivity to CpG oligodeoxynucleotides. *J*  
610 *Immunol* **168**, 4531-4537 (2002).  
611
- 612 40. Eigenbrod, T., Pelka, K., Latz, E., Kreikemeyer, B. & Dalpke, A.H. TLR8 Senses Bacterial RNA  
613 in Human Monocytes and Plays a Nonredundant Role for Recognition of *Streptococcus*  
614 *pyogenes*. *J Immunol* **195**, 1092-1099 (2015).  
615
- 616 41. Bergstrom, B. *et al.* TLR8 Senses *Staphylococcus aureus* RNA in Human Primary Monocytes  
617 and Macrophages and Induces IFN-beta Production via a TAK1-IKKbeta-IRF5 Signaling  
618 Pathway. *J Immunol* **195**, 1100-1111 (2015).  
619
- 620 42. Meurens, F., Summerfield, A., Nauwynck, H., Saif, L. & Gerdts, V. The pig: a model for human  
621 infectious diseases. *Trends Microbiol* **20**, 50-57 (2012).  
622
- 623 43. Mair, K.H. *et al.* The porcine innate immune system: an update. *Dev Comp Immunol* **45**, 321-343  
624 (2014).  
625
- 626 44. Zhu, J., Lai, K., Brownile, R., Babiuk, L.A. & Mutwiri, G.K. Porcine TLR8 and TLR7 are both  
627 activated by a selective TLR7 ligand, imiquimod. *Mol Immunol* **45**, 3238-3243 (2008).  
628
- 629 45. Lindner, T., Springer, S., Selbitz, H.J. . The use of a *Salmonella Typhimurium* live vaccine to  
630 control *Salmonella Typhimurium* in fattening pigs in field and effects on serological surveillance.  
631 *Proceedings of the 7th International Safepork Symposium on Epidemiology and Control of*  
632 *Foodborne Pathogens in Pork, Verona, Italy, 237 - 239* (2007).  
633
- 634 46. Sinkora, M., Stepanova, K. & Sinkorova, J. Different anti-CD21 antibodies can be used to  
635 discriminate developmentally and functionally different subsets of B lymphocytes in circulation  
636 of pigs. *Dev Comp Immunol* **39**, 409-418 (2013).  
637
- 638 47. Oh, D.Y. *et al.* A functional toll-like receptor 8 variant is associated with HIV disease restriction.  
639 *J Infect Dis* **198**, 701-709 (2008).

- 640  
641 48. Wang, C.H. *et al.* TLR7 and TLR8 gene variations and susceptibility to hepatitis C virus  
642 infection. *PLoS One* **6**, e26235 (2011).  
643
- 644 49. Tanji, H., Ohto, U., Shibata, T., Miyake, K. & Shimizu, T. Structural reorganization of the Toll-  
645 like receptor 8 dimer induced by agonistic ligands. *Science* **339**, 1426-1429 (2013).  
646
- 647 50. Davila, S. *et al.* Genetic association and expression studies indicate a role of toll-like receptor 8 in  
648 pulmonary tuberculosis. *PLoS Genet* **4**, e1000218 (2008).  
649
- 650 51. Dowling, D.J. *et al.* Toll-like receptor 8 agonist nanoparticles mimic immunomodulating effects  
651 of the live BCG vaccine and enhance neonatal innate and adaptive immune responses. *J Allergy*  
652 *Clin Immunol* (2017).  
653
- 654 52. Dowling, D.J. *et al.* TLR7/8 adjuvant overcomes newborn hyporesponsiveness to pneumococcal  
655 conjugate vaccine at birth. *JCI Insight* **2**, e91020 (2017).  
656
- 657 53. Wille-Reece, U. *et al.* HIV Gag protein conjugated to a Toll-like receptor 7/8 agonist improves  
658 the magnitude and quality of Th1 and CD8+ T cell responses in nonhuman primates. *Proc Natl*  
659 *Acad Sci U S A* **102**, 15190-15194 (2005).  
660
- 661 54. Colditz, G.A. *et al.* Efficacy of BCG vaccine in the prevention of tuberculosis. Meta-analysis of  
662 the published literature. *JAMA* **271**, 698-702 (1994).  
663
- 664 55. Achkar, J.M. & Casadevall, A. Antibody-mediated immunity against tuberculosis: implications  
665 for vaccine development. *Cell Host Microbe* **13**, 250-262 (2013).  
666
- 667 56. Skogmar, S. *et al.* CD4 cell levels during treatment for tuberculosis (TB) in Ethiopian adults and  
668 clinical markers associated with CD4 lymphocytopenia. *PLoS One* **8**, e83270 (2013).  
669
- 670 57. Kumar, N.P. *et al.* Decreased frequencies of circulating CD4(+) T follicular helper cells  
671 associated with diminished plasma IL-21 in active pulmonary tuberculosis. *PLoS One* **9**, e111098  
672 (2014).  
673
- 674 58. Li, L. *et al.* Mycobacterium tuberculosis-Specific IL-21+IFN-gamma+CD4+ T Cells Are  
675 Regulated by IL-12. *PLoS One* **11**, e0147356 (2016).  
676
- 677 59. Pulendran, B., Oh, J.Z., Nakaya, H.I., Ravindran, R. & Kazmin, D.A. Immunity to viruses:  
678 learning from successful human vaccines. *Immunol Rev* **255**, 243-255 (2013).  
679
- 680 60. Fairbairn, L., Kapetanovic, R., Sester, D.P. & Hume, D.A. The mononuclear phagocyte system of  
681 the pig as a model for understanding human innate immunity and disease. *J Leukoc Biol* **89**, 855-  
682 871 (2011).  
683
- 684 61. Landers, T.F., Cohen, B., Wittum, T.E. & Larson, E.L. A review of antibiotic use in food  
685 animals: perspective, policy, and potential. *Public Health Rep* **127**, 4-22 (2012).  
686
- 687 62. Helbig, E.T., Opitz, B. & Sander, L.E. Adjuvant immunotherapies as a novel approach to  
688 bacterial infections. *Immunotherapy* **5**, 365-381 (2013).  
689

690 63. Brahmakshatriya, V. *et al.* IL-6 Production by TLR-Activated APC Broadly Enhances Aged  
691 Cognate CD4 Helper and B Cell Antibody Responses In Vivo. *J Immunol* **198**, 2819-2833  
692 (2017).  
693

694 64. Havenar-Daughton, C. *et al.* Direct Probing of Germinal Center Responses Reveals  
695 Immunological Features and Bottlenecks for Neutralizing Antibody Responses to HIV Env  
696 Trimer. *Cell Rep* **17**, 2195-2209 (2016).  
697

698 65. Havenar-Daughton, C. *et al.* Cytokine-Independent Detection of Antigen-Specific Germinal  
699 Center T Follicular Helper Cells in Immunized Nonhuman Primates Using a Live Cell  
700 Activation-Induced Marker Technique. *J Immunol* **197**, 994-1002 (2016).  
701

702 66. Lee, B.R. *et al.* Combination of TLR1/2 and TLR3 ligands enhances CD4(+) T cell longevity and  
703 antibody responses by modulating type I IFN production. *Sci Rep* **6**, 32526 (2016).  
704

705 67. Martins, K.A. *et al.* Adjuvant-enhanced CD4 T Cell Responses are Critical to Durable Vaccine  
706 Immunity. *EBioMedicine* **3**, 67-78 (2016).  
707

708 68. Poteet, E. *et al.* Toll-like receptor 3 adjuvant in combination with virus-like particles elicit a  
709 humoral response against HIV. *Vaccine* **34**, 5886-5894 (2016).  
710

711 69. Soni, C. *et al.* B cell-intrinsic TLR7 signaling is essential for the development of spontaneous  
712 germinal centers. *J Immunol* **193**, 4400-4414 (2014).  
713

714 70. Chakarov, S. & Fazilleau, N. Monocyte-derived dendritic cells promote T follicular helper cell  
715 differentiation. *EMBO Mol Med* **6**, 590-603 (2014).  
716

717 71. Heil, F. *et al.* Species-specific recognition of single-stranded RNA via toll-like receptor 7 and 8.  
718 *Science* **303**, 1526-1529 (2004).  
719

720 72. Hochrein, H. *et al.* Interleukin (IL)-4 is a major regulatory cytokine governing bioactive IL-12  
721 production by mouse and human dendritic cells. *J Exp Med* **192**, 823-833 (2000).  
722

723 73. de Beaucoudrey, L. *et al.* Revisiting human IL-12Rbeta1 deficiency: a survey of 141 patients  
724 from 30 countries. *Medicine (Baltimore)* **89**, 381-402 (2010).  
725

726 74. Picard, C. *et al.* Clinical features and outcome of patients with IRAK-4 and MyD88 deficiency.  
727 *Medicine (Baltimore)* **89**, 403-425 (2010).  
728

729 75. Ma, C.S. *et al.* Functional STAT3 deficiency compromises the generation of human T follicular  
730 helper cells. *Blood* **119**, 3997-4008 (2012).  
731

732 76. Ma, C.S. *et al.* Monogenic mutations differentially affect the quantity and quality of T follicular  
733 helper cells in patients with human primary immunodeficiencies. *J Allergy Clin Immunol* **136**,  
734 993-1006 e1001 (2015).  
735

736 77. Rao, D.A. *et al.* Pathologically expanded peripheral T helper cell subset drives B cells in  
737 rheumatoid arthritis. *Nature* **542**, 110-114 (2017).  
738  
739 .  
740

741  
742



743 **Materials and Methods**

744 *Cell isolation and culture*

745 Human monocytes, T cells and B cells used in this study were either freshly isolated from  
746 peripheral venous blood of healthy volunteers or from buffy coats obtained from the German Red  
747 Cross Blood Transfusion Service, Berlin, Germany. Permission for experiments with human  
748 primary cells was obtained from the local ethic committee. Peripheral blood mononuclear cells  
749 (PBMC) were isolated by density gradient centrifugation over Histopaque-1077 (Sigma-Aldrich;  
750 Steinheim, Germany). CD14<sup>+</sup>CD16<sup>-</sup> monocytes were purified by negative selection via  
751 immunomagnetic separation using EasySep monocyte isolation kits with CD16 depletion  
752 (Stemcell Technologies; Grenoble, France) according to the manufacturer's instructions. Isolated  
753 monocytes were cultured at a density of 1 x 10<sup>6</sup> cells/ml in RPMI1640 supplemented with 10%  
754 fetal calf serum (FCS), 1% glutamine, 1% HEPES buffer, 1% non-essential amino acids (all from  
755 Sigma-Aldrich). T cells were cultured in RPMI1640 supplemented with 10% human serum (from  
756 the respective T cell donor), 1% glutamine, 1% HEPES buffer, 1% non-essential amino acids,  
757 some T cell conditions were supplemented with 2,5ng/ml of TGF- $\beta$  (eBioscience, San Diego, CA).  
758 All cells were grown at 37°C, 5% CO<sub>2</sub> in a humidified incubator.

759 Untouched human CD1<sup>+</sup> mDC were purified by negative selection via immunomagnetic bead  
760 separation (Miltenyi Biotec, Bergisch Gladbach, Germany) following the manufacturer's  
761 instructions.

762 Naïve CD4<sup>+</sup> T cells were purified by immunomagnetic separation using negative selection  
763 (MagneSort™ Human CD4 Naïve T cell Enrichment Kit, eBioscience, San Diego, CA ). Total  
764 CD4<sup>+</sup> T cells (used in Figure 3A, B and D, and Fig. 4F and G and fig. S3) were isolated by magnetic  
765 separation using negative selection (MagneSort™ Human CD4 T cell Enrichment Kit,  
766 eBioscience).

767 Untouched naïve human B cells were isolated by immunomagnetic bead separation (Miltenyi  
768 Biotec, Bergisch Gladbach, Germany) following the manufacturer's instructions.

769 Cell purity was routinely checked by flow cytometry and only purities of >85% (monocytes) and  
770 >95% (T and B) cells were used for subsequent experiments.

771

772 *Bacteria and infection*

773 *Escherichia coli* K12, strain DH5 $\alpha$ , thymidine auxotrophs (*thyA*<sup>-</sup>) were selected as previously  
774 described<sup>4</sup>. Auxotrophy was confirmed by inoculation and overnight culture of single colonies in  
775 LB medium. *ThyA*<sup>-</sup> *E. coli* (hereafter referred to as EC) grew only in the presence of thymidine  
776 and were resistant to trimethoprim. For phagocytosis experiments, EC were grown to mid-log  
777 phase, washed twice in phosphate buffered saline (PBS) to remove thymidine and LB salts before  
778 addition to cells. For heat killing, EC were grown to log phase, washed and re-suspended in PBS  
779 at an optical density at 600nm (OD<sub>600</sub>) of 0.6, and subsequently incubated at 60 °C for 90 min.  
780 Heat-killed *thyA*<sup>-</sup> *E. coli* (HKEC) were used immediately after killing or stored at -80 °C for up to  
781 three months. Efficient killing was confirmed by overnight plating on thymidine/trimethoprim-  
782 supplemented LB-agar plates. Alternatively, *Bacillus subtilis* strain 168 was used for analogous  
783 infection experiments. For heat killing, *B. subtilis* were grown to mid-log phase, washed and re-  
784 suspended in PBS at an optical density at 600nm (OD 600) of 0.6, and subsequently incubated at  
785 95°C for 30min. Efficient killing was confirmed by overnight plating on LB-agar plates. . For heat  
786 killing, *S. enterica* serovar Typhimurium were grown to mid-log phase, washed and re-suspended  
787 in PBS at an optical density at 600nm (OD 600) of 0.6, and subsequently incubated at 95°C for  
788 30min. Efficient killing was confirmed by overnight plating on LB-agar plates. Infection of human  
789 monocyte was performed at the indicated multiplicities of infection (MOI).

790 BCG was grown in Middlebrook 7H9 medium supplemented with 0.05% Tween 80. For  
791 phagocytosis experiments, BCG were grown to mid-log phase, washed once in phosphate buffered  
792 saline (PBS) and resuspended in complete cell culture media via repeated tuberculin type needle  
793 passages (10x). For heat killing, BCG were grown to log phase and incubated at 60°C for 90min.  
794 Heat-killed BCG (HKBCG) were used immediately after killing. Efficient killing was confirmed  
795 by 96h inoculation in competent media.

796 *Co-culture assays*

797 For monocyte : T cell co-cultures monocytes were cultured as described above and stimulated as  
798 indicated (e.g. EC, HKEC MOI 1-25) in antibiotic-free medium. After one and a half hours,  
799 penicillin/streptomycin (1%) was added together with autologous naïve CD4<sup>+</sup> T cells at a  
800 monocyte to T cell ratio of 2:1 and staphylococcal enterotoxin B (SEB, Sigma) at a concentration  
801 of 1.0 $\mu$ g/ml. After 5 days of co-culture T cells were harvested, washed, restimulated with Phorbol-

802 12-myristat-13-acetat (PMA, 50ng/ml) and Ionomycin (1µg/ml, both obtained from Sigma),  
803 stained and analyzed by flow cytometry.

804 For T : B cell co-cultures, T cells were differentiated by co-cultures with autologous monocytes  
805 for 6 days as described before. CXCR5<sup>+</sup>ICOS<sup>+</sup>PD-1<sup>hi</sup> T cells were sorted by flow cytometry (BD  
806 FACS-Aria II) and added to naïve autologous B cells at a T to B cell ratio of 1:2 in the presence  
807 of SEB (1µg/ml). After 12 days co-culture B and T cells were harvested and analyzed by flow  
808 cytometry. For analysis of plasma blast differentiation, sorted T<sub>FH</sub> (CD19<sup>-</sup> CD4<sup>+</sup> CD45RA<sup>-</sup>  
809 CXCR5<sup>+</sup>) or naive (CD19<sup>-</sup> CD4<sup>+</sup> CD45RA<sup>+</sup>) T cells were cocultured with memory B cells at a ratio  
810 of 1:1 in the presence of 4 ng/ml SEB for 7 days.

### 811 *Antibodies and reagents*

812 Antibodies for flow cytometry: CD3 (UCHT1, cat.: 300415), CD4 (OKT4, cat.: 317424), IFN $\gamma$   
813 (4S.B3, cat.: 502528), IL17 (BL168, cat.: 512306), CXCR5 (J252D4, cat.: 356904), PD1  
814 (EH12.2H7, cat.: 329922), ICOS (C398.4A, cat.: 313510), CD19 (HIB19, cat.: 302228 or SJ25C1,  
815 cat.: 363022), CD20 (2H7, cat.: 302324), CD27 (O323, cat.: 302810), CD38 (HIT2, cat.: 303516  
816 or or M-T271, cat.: 356418), IgM (MHM-88, cat.: 314520), IgD (IA6-2, cat.: 348216), MHC2  
817 (L243, cat.: 307610), anti IL-1b (H1B-27, cat.: 511604), Zombie violet (cat.: 423113;(all from  
818 Biolegend, San Diego, CA). Anti IFN $\alpha$  (polyclonal , cat.: ab10739, Abcam, Cambridge, UK),  
819 BCL6 (K112-91, cat.: 561522/ 561525, BD, Franklin Lake, NJ), IL-21 (ebio3A3-N2, cat.: 50-  
820 7219, eBioscience), CD14 (TÜK4, cat.: 130-096-875, Miltenyi Biotec, Bergisch Gladbach,  
821 Germany), CD38 (OKT 10, CRL-8022, ATCC, Manassas, VA).porcine Monocyte/Granulocyte  
822 (74-22-15A, cat.: 561499, BD, Franklin Lake, NJ), porcine CD3 (BB23-8E6-8C8, cat.: 561478),  
823 porcine CD4 (74-12-4-RUO, cat.: 561472, BD), porcine CD8b (295/33-25, cat.: 561484, BD),  
824 IL-21 (polyclonal, cat.: orb9043, Biorbyt, San Francisco, CA) porcine CD8a (76-2-11, cat.:  
825 561475, BD), porcine CD2 (MSA4, cat.: WS0590S-100, Kingfisher Biotech), porcine SLA Class  
826 II DR (2E9/13, cat.: MCA2314F, AbD Serotec), porcine CD21 (BB6-11C9.6, cat.: SBA-4530-09,  
827 Southern Biotech), porcine TCR1  $\delta$  (PGBL22A, cat.: WS0621S-100, Kingfisher Biotech),  
828 mouse-IgG (Poly4053, cat.: 405317, Biolegend), porcine IgM (polyclonal, cat.: AAI48B, Bio-  
829 Rad), Streptavidin (cat.: 25-4317-82, eBioscience), Foxp3 (FJK-16s, cat.: 48-5773-82,  
830 eBioscience), Tbet (eBio4B10, cat.: 12-5825-82, eBioscience). Fixable Viability Dyes (cat.: 65-  
831 0865-14 and 65-0866-14, eBioscience).

832 Neutralizing antibodies: anti-IL-6 (6708, cat.: MAB206-SP, R&D Systems, Minneapolis, MN),  
833 anti-IL-12 (B-T21, cat.: BMS152, eBioscience) and anti-TNF $\alpha$  (MAB11, cat.: 502901, Biolegend)  
834 were used at 10 $\mu$ g/ml. Anti-IL-27 (307426, cat.: MAB25261 F, R&D Systems) was used at  
835 5 $\mu$ g/ml.

836 Recombinant cytokines: rIL-12 (eBioscience) was used at 100pg/ml, rTNF, rIL-6 (eBioscience),  
837 rIL-27 (R&D Systems) were used at 10 ng/ml.

838 TLR ligands were purchased from Invivogen (Toulouse, France) and used at the indicated  
839 concentration: CL075 (3M002; 1 $\mu$ g/ml), LPS-EK Ultrapure (2 $\mu$ g/ml), Pam3CSK4 (200ng/ml),  
840 Poly(I:C) LMW (2 $\mu$ g/ml), ODN 2395 (5 $\mu$ M). Bacterial RNA was isolated from mid-log phase  
841 cultures of DH5alpha *E. coli* using Trizol (Life Technologies, Karlsruhe, Germany). Transfection  
842 of bacterial RNA into human monocytes was performed using polycationic polypeptide poly-L -  
843 arginine (pLa) (Sigma-Aldrich).

#### 844 *Enzyme-linked immunosorbent assay (ELISA)*

845 TNF, IL-1 $\beta$ , IL-6, IL-10, IL-12p40, IL-23, GM-CSF and IL-27 concentrations in culture  
846 supernatants were measured by ELISA (all purchased from eBioscience) according to standard  
847 manufacturer's recommendations. Concentrations of IL-12p70 were measured using human IL-  
848 12p70 High Sensitivity ELISA kit (eBioscience). The samples were analyzed for absorbance at  
849 450 nm using FilterMax F5 Multi-Mode Microplate Reader (Molecular Devices, Biberach an der  
850 Riss, Germany). Porcine IL-12p40 and IL-6 concentrations in culture supernatants were measured  
851 by ProcartaPlex Pig Kit (eBioscience) or by Quantikine ELISA kit (R&D Systems) and results  
852 were collected using a Luminex MAGPIX instrument (Merck Millipore, Billerica, MA). Human  
853 IgG was determined by ELISA using polyclonal goat anti-human IgG (TAGO Immunologicals,  
854 Burlingame, CA) and purified human IgG as standard. Results were collected on a Spark  
855 multimode reader (Tecan, Männedorf, Switzerland).

#### 856 *Anti-S. enterica IgG ELISA*

857 96-well microtiter plates were coated overnight with *S. enterica* serovar Typhimurium  
858 (**Salmoporc-STM**) lysates (3 $\mu$ g/ml) that we generated from log-phase cultures of *Hys<sup>-</sup>Ade<sup>-</sup> S.*  
859 *enterica*. Serum samples from immunized pigs were serially diluted (12 dilutions) and incubated  
860 in the pre-coated plates for 12 h at 4 °C followed by washing and incubation with goat anti-pig IgG  
861 (gamma)-HRP (SeraCare Life Sciences, Milford, MA) for 1 h. Bound goat anti-pig IgG (gamma)-

862 HRP was visualized by the addition of TMB substrate (Thermo Fisher), and the anti-*S. enterica*  
863 antibody titers for each animals were visualized as absorbance readings at 450nm at a set serum  
864 dilution of 1 to 51200.

#### 865 *RNA Isolation*

866 CD14<sup>+</sup>CD16<sup>-</sup> human monocytes were sorted by flow cytometry and were infected with EC at  
867 MOI=10 or stimulated with HKEC at 10:1 ratio of bacteria to cells. After 6 hours, cells were  
868 harvested, washed once in PBS, and lysed in Trizol (Life Technologies). Total RNA was prepared  
869 according to the manufacturer's suggested protocol.

#### 870 *Gene Array*

871 Total RNA was prepared from four independent experiments (= four separate donors) according  
872 to the Trizol manufacturer's protocol. Samples were further purified on columns (RNeasy Micro  
873 Kit, Qiagen, Hilden, Germany).

874 RNA integrity was checked on an Agilent 2100 Bioanalyser (Agilent Technologies, Santa Clara,  
875 CA) with 6000 Nano Chips. RNA was judged as suitable only if samples showed intact bands of  
876 18S and 28S ribosomal RNA subunits, displayed no chromosomal peaks or RNA degradation  
877 products, and had a RNA integrity number (RIN) above 8.0.

878 One-hundred nanograms of RNA were used for whole-transcript cDNA synthesis with the Ambion  
879 WT expression kit (Life Technologies). Hybridization, washing and scanning of an Affymetrix  
880 GeneChip Human Gene 1.1 ST 24-array plate was carried out according to standard Affymetrix  
881 protocols on a GeneTitan instrument (Affymetrix, Santa Clara, CA).

882 Quality control, normalization and statistical analysis was performed using MADMAX, a pipeline  
883 consisting of integrated Bioconductor packages<sup>78</sup>. Probe sets were redefined according to Dai *et*  
884 *al.* using current genome information<sup>79</sup>. Normalized gene expression estimates were obtained from  
885 the raw intensity values by using the robust multiarray analysis preprocessing algorithm available  
886 in the library "AffyPLM" using default settings<sup>80</sup>. Only genes that were targeted by at least 7  
887 probes, reached log<sub>2</sub> expression level of >4.32 on at least three microarrays and had a log<sub>2</sub>  
888 interquartile range value >0.25 across all samples were considered for further analysis. Intensity-  
889 based moderated t-statistics were applied for pairwise comparisons to identify differentially

890 regulated genes<sup>81</sup>. To correct for multiple testing a false discovery rate method was used to  
891 calculate q-values<sup>82</sup>. A q-value < 0.01 was considered significant.

892 *RNA interference*

893 Silencer Select siRNA duplexes targeting TLR8 (sequence ID: s27920, s27921 and s27922),  
894 MyD88 (sequence ID: s9136, s9137 and s9138) and negative controls were obtained from Life  
895 Technologies. Monocytes cultured in 96-well plates were transfected with 25nM of each siRNA  
896 using Viromer Blue transfection reagent (Lipocalyx, Leipzig, Germany) following manufacturer  
897 recommendations for sensitive cells and reverse transfection. Cells were plated at a density 5x10<sup>5</sup>  
898 cells/ml in a final volume of 100µl in 96 well plates. Forty-eight hours post transfection cells were  
899 infected or treated as described. Knockdown of TLR8 and Myd88 was confirmed 48 hours after  
900 siRNA transfection by RT-PCR using specific primers (TLR8: forward primer 5'-  
901 AgTTTCTCTTCTCggCCACC-3' and reverse primer, 5'-ACATgTTTTCCATgTTTCTgTTgT -3',  
902 MyD88: forward primer 5'-TCTCCAaggTgCCCATCAGAA-3' and reverse primer 5'-  
903 ggTTggTgTAgTCgCAgACA-3').

904 Four Custom designed Silencer Select siRNA duplexes targeting porcine TLR8 (combination of  
905 four siRNA duplexes) were purchased from Life Technologies with sequences:

906 TLR8-1 sense: 5'-GCAAAUUGAUUUUACCAUUTT-3';

907           antisense: 5'-AAUGGUAAAAUCAAUUUGCTT-3';

908 TLR8-2 sense: 5'-GAUUUAAGCUUGAACAGUATT-3';

909           antisense: 5'-UACUGUUCAAGCUUAAAUCTA-3';

910 TLR8-3 sense: 5'-GCAUCUUUACUUUAAACAGATT-3';

911           antisense: 5'-UCUGUUAAGUAAAGAUGCTG-3';

912 TLR8-4 sense: 5'-CAAUAUUCGUUUUAACCAATT-3';

913           antisense: 5'-UUGGUUAAAACGAAUAUUGTC-3';

914 Porcine CD14<sup>+</sup> monocytes cultured in 96-well plates were transfected with 25nM of each siRNA  
915 folloing the protocol described above for human cells. Forty-eight hours post transfection cells  
916 were infected or treated as described.

917 *Flow cytometry and cell sorting*

918 Flow cytometry regularly was performed on a BD FACS Canto II cytometer Data was analyzed  
919 using FlowJo software (Treestar, San Carlos, CA).

920 CD14<sup>+</sup>CD16<sup>-</sup> monocytes were sorted from PBMCs on a BD Aria II SORP cell sorter (BD  
921 Biosciences) CD4<sup>+</sup>CXCR5<sup>+</sup> and CD4<sup>+</sup>CXCR5<sup>-</sup> T cells were sorted from monocyte : T cell co-  
922 cultures on a BD Aria II SORP cell sorter. In vitro generated Tfh cells were sorted on an ARIA II  
923 sorter as CD19<sup>-</sup> CD4<sup>+</sup> CD45RA<sup>-</sup> CXCR5<sup>+</sup> and naive T cells as CD19<sup>-</sup> CD4<sup>+</sup> CD45RA<sup>+</sup>. Memory B  
924 cells were sorted from human tonsils as CD4<sup>-</sup> CD19<sup>+</sup> IgD<sup>-</sup> CD38<sup>-</sup> cells. Cell purity checks were  
925 performed and a purity of >97% was confirmed.

926 *QuantiGene Plex transcript analysis*

927 Quantigene multiplex-plex assay (Affymetrix,) was performed to quantify the expression of the  
928 following genes *GATA3*, *MAF*, *IL21*, *TBX21*, *RORC*, *FOXO1*, *BCL6* and two housekeeper genes  
929 (*ACTB* and *HPRT1*) according to the manufacturer's protocol. In brief, CD4<sup>+</sup> T cells were lysed at  
930 a concentration of 500 cell/μl of lysis mixture supplemented with proteinase K and incubated at  
931 50°C for 30 min, prior to addition to a hybridization plate. The hybridization plate was sealed with  
932 heat-sealing foil and placed in a shaking incubator (VorTemp 56) at 54±1°C and 600 rpm to allow  
933 the samples to hybridize for 18-22 h. Fluorescent bead signal detection was obtained using Bio-  
934 Plex Suspension Array System (Bio-Rad Laboratories, Hercules, CA). The mean fluorescent  
935 intensity for each probe was recorded.

936 *Animal experiment*

937 The animal experiments were performed in accordance with the Danish Animal Welfare Act under  
938 approval and authorization issued by the Danish Animal Experiment Inspectorate.

939 In total, 18 five-week-old pigs (Danish Landrace/Danish Yorkshire crossbreeds, paternal lineage  
940 Duroc) of both sexes, raised on a commercial farm (Bøgekærgård, Faxe, Denmark) were stratified  
941 by size (6.3 to 10.4 kg, averaging 8.0 kg) and sex, and distributed to three groups. Animals in each  
942 group received 1 ml subcutaneous vaccination in the right side of the neck as follows: 1) live  
943 *Salmonella enterica* serovar Typhimurium vaccine (Salmoporc STM Ch.-B. 022 07 15, IDT  
944 Biologika, Dessau-Roßlau, Germany) containing 3.32 x 10<sup>8</sup> CFU per dose, according to the  
945 product insert); 2) heat-inactivated (65° for 90 minutes) Salmoporc STM vaccine (HKST) using

946 the same dose as in 1); 3) saline alone. The live vaccine was administered within 2h of  
947 reconstitution. The same immunization regimen was repeated as booster injections on day 14.  
948 Heat-killing of the vaccine was confirmed by absence of bacterial growth on LB plates incubated  
949 at 37°C for 24h. Throughout the experiment the pigs were housed in two adjoining boxes equally  
950 mixed across the 3 treatment groups. One pig in the live vaccine group was euthanized on day 19  
951 of the experiment due to severe umbilical hernia, unrelated to the vaccine. One pig in the control  
952 group presented on day 0 of the experiment with fever, dyspnea and generalized fatigue, suspected  
953 of pneumonia, and was therefore treated successfully with 160 mg benzylpenicillin and 200 mg  
954 dihydrostreptomycin (0.8 ml Streptocillin Vet) over 3 consecutive days. It was excluded from the  
955 analysis. Five animals per group were included in the final analyses.

956 Animals were sacrificed according to regulations. Transverse sections of spleen and prescapular  
957 lymph node (LN, *cervicalis superficialis dorsalis*) draining from the injection site were fixated in  
958 10% neutral-buffered formalin (4% formaldehyde, Pioneer Research Chemicals Ltd) for  
959 immunohistochemistry. The remaining LN and spleen tissues samples were homogenized using  
960 disposable scalpels and single-cell suspensions were isolated by forcing homogenized tissue  
961 samples through a cell strainer (70 µm, Greiner Bio-One, Kremsmünster, Austria), followed by  
962 two washes with RPMI 1640 and subsequently cultured in RPMI1640 supplemented with 10%  
963 fetal calf serum (FCS), 1% glutamine, 1% HEPES buffer, 1% non-essential amino acids (all from  
964 Sigma-Aldrich).

965 For BCG vaccination 12 female pigs (Danish Landrace/Danish Yorkshire crossbreeds and paternal  
966 Duroc) were delivered after weaning to the research facilities at the National Veterinary Institute,  
967 Technical University of Denmark, Frederiksberg, Denmark from a commercial farm (Askelygård,  
968 Roskilde, Denmark). At 5 weeks of age the pigs were stratified by size (total weight range 5.5-  
969 11.5 kg, mean 8.9 kg) and allocated to two vaccination groups, receiving either 1.5-2 vials of BCG  
970 (Statens Serum Institut, Copenhagen, Denmark) resuspended in 0.8ml Sauton diluent (~15-20  
971 times a standard BCG dose) or 1.0ml Sauton diluent alone, applied by three adjacent injections  
972 s.c. in the right hind leg by a midwife with extensive experience in BCG vaccination of human  
973 newborns. 24 days after vaccination, venous blood was collected into EDTA containing tubes, the  
974 pigs were sacrificed according to regulations, and the spleens were retrieved and preserved in cold



975 RPMI-1640 Glutamax supplemented with penicillin and streptomycin (all Gibco, city, country)  
976 for subsequent processing.

977 For *in vitro* experiments reported in Fig. 7 and Supplementary Figure 4 spleens samples were  
978 collected from German Landrace pigs of both sexes aged between 8 weeks and 1 year. Single cell  
979 suspensions were prepared as described above.

980 Splenocytes were cultured in IMDM (Pan-biotech, Aidenbach, Germany) supplemented with 10%  
981 FCS and stimulated with ST, HKST (MOI 0.1, 0.5, 1, 3), LPS (2µg/ml), CL075 (1µg/ml) or  
982 pLa+RNA (280ng and 237ng respectively) in the presence of Concavalin A (2µg/ml)  
983 (Fisherscientific, Schwerte, Germany). After one hour penicillin/streptomycin (1%) was added.  
984 After 4 days cells were restimulated with Phorbol-12-myristat-13-acetat (PMA, 50ng/ml) and  
985 Ionomycin (1µg/ml, both obtained from Sigma) and then harvested, washed and analyzed by flow  
986 cytometry. Live and dead cells were discriminated using Zombie Violet Fixable Viability Kit  
987 (Biolegend), dead cells were excluded from the analysis.

#### 988 *Immunohistochemistry*

989 Spleen samples were immersion-fixed in formalin and embedded in paraffin, cut in 2 µm sections  
990 for immunohistochemical analyses after dewaxing in xylene and rehydration in decreasing ethanol  
991 concentrations. For detection of PAX5, KI67 and BCL22, heat-mediated antigen retrieval was  
992 performed in 10 mM citric acid (pH 6.0), microwaved at 600 W for 12 min. Spleen sections were  
993 incubated with a purified mouse antibody monoclonal to PAX5 (1:400, clone 24/Pax5, BD  
994 Biosciences, Heidelberg, Germany) or BCL2 (1:100, LS-B2352, LSBio, Seattle, WA, USA) or  
995 with a purified rabbit antibody monoclonal to KI67 (1:150, clone SP6, Cell Marque, Rocklin, CA,  
996 USA) at 4°C overnight. Incubation with an irrelevant immuno-purified mouse or rabbit antibody  
997 at the same dilution served as negative controls. Slides were incubated with biotinylated, secondary  
998 goat anti-mouse IgG (1:200, BA 9200, Vector Burlingame, CA) or goat anti-rabbit IgG (1:200,  
999 BA 1000, Vector, Burlingame, CA) antibodies and HRP-coupled streptavidin. Diaminobenzidine  
1000 (DAB) was used as substrate for color development. All slides were counterstained with  
1001 hematoxylin, dehydrated through graded ethanols, cleared in xylene and coverslipped. Whole slide

1002 images of spleen tissues were generated by Aperio CS2 digital pathology scanner (Leica  
1003 Biosystems Imaging Inc., Vista, CA, USA).

#### 1004 *Immunofluorescence*

1005 For immunofluorescent co-staining of **PAX5** and **KI67**, slides were incubated with the purified  
1006 mouse antibody monoclonal to **PAX5** (1:50) over night at 4°C as described above and with Alexa  
1007 Fluor 568-conjugated, secondary goat anti-mouse IgG antibody (1:200, Thermo Fisher Scientific,  
1008 Darmstad, Germany) for 45 min. at room temperature. Slides were then incubated with a purified  
1009 rat antibody monoclonal to **KI67** (1:100, clone SolA15, eBioscience) at 4°C over night, incubated  
1010 with Alexa Fluor 488-conjugated, secondary goat anti-rat IgG antibody (1:200, Thermo Fisher  
1011 Scientific) for 45 min. at room temperature and mounted with Roti-Mount Fluor-Care DAPI (4,6-  
1012 diaminidino-2-phenylindole, Carl Roth, Karlsruhe, Germany). Adequate negative controls,  
1013 including incubation of slides with only one primary but both secondary antibodies, were  
1014 conducted. Slides were analyzed by immunofluorescence microscopy with an Olympus BX41  
1015 microscope equipped with a DP80 camera (Olympus, Hamburg, Germany).

#### 1016 *Case-Control Study*

1017 Samples of TB patients and healthy volunteers were collected in Mahavir Hospital, Hyderabad  
1018 (India) and the generated cohort has been described before<sup>83</sup>. Informed consent was obtained from  
1019 all individuals, and all investigations were conducted according to the principles of the Helsinki  
1020 Declaration. Written approval was obtained from the research ethics board of the Central  
1021 University of Hyderabad and Mahavir Hospital. Patients were enrolled in the Revised National  
1022 Tuberculosis Control Program (RNTCP) of India, and recruited into the study on the day of  
1023 treatment initiation (according to DOTS strategy). HIV-positive and relapse cases were excluded  
1024 from the cohort. TB diagnosis was based on clinical examination, chest X-Ray, positive sputum  
1025 test or histopathology. Healthy household contacts of the TB patients were recruited as controls,  
1026 to ensure comparable exposure rates and environmental conditions. BCG vaccination status was  
1027 determined by the presence of a BCG-related skin scar. The cohort consisted of 293 patients and  
1028 165 controls. 61,4% of the TB patients had pulmonary TB (PTB) and 38.6% extra-pulmonary TB  
1029 (ETB). Controls were significantly older (mean=34.2±9.3) than patients (mean=25.4±10,4;t(456)=  
1030 8.787;p<0.0001) and had a significantly higher mean BMI (mean=23.8±4.9 and mean=18.0±4.1  
1031 respectively, t(292.8)=12.995;p<.0001). Gender distribution did not differ significantly between

1032 controls (59.4% females) and patients (61.8% females). The age and BMI differences were  
1033 corrected for using a binary logistic regression model.

#### 1034 *SNP Analysis*

1035 DNA of all study subjects was extracted from buccal swabs using FlexiGene DNA extraction Kit  
1036 (Qiagen). TLR8 SNPs were analyzed by real-time PCR on a Light Cycler instrument (Roche,  
1037 Mannheim, Germany) using the following PCR primer sets:

1038 forward 5'-TCAGGAAGTTAGCCAGTTTCTC-3',

1039 reverse 5'-CCTGCATTTACAGTTGTTTCGAT-3',

1040 sensor 5'-AAATAGAAGTGGCTTACCACGTTTCTG-3'T-FITC,

1041 anchor Cy5-5'-TTCTAATTTTTCATTCCGTAAGTTGCAGCAGCGCA-3'.

1042 Based on previous observations that the presence of an A defines the functionality, we defined the  
1043 A/AA/AG as TLR8-A, and G/GG as TLR8-G status for our analysis.

1044

#### 1045 *Statistical Analysis*

1046 Statistical analyses of in vitro experiments were performed using one-way-ANOVA test and  
1047 Holm-Sidak's multiple comparisons test, or 2way-ANOVA, or Wilcoxon's matched-pairs signed  
1048 rank test, or linear regression analysis where appropriate. Calculations were performed using  
1049 GraphPad Prism 6 Software (GraphPad Software, La Jolla, CA, USA)

1050 For all statistical analysis a p-value <0.05 was considered statistically significant. 95% Confidence  
1051 Intervals are given in squared brackets in tables S3-S4 [CI 95%]. Baseline characteristics of the  
1052 study population were analyzed using student's t-test or Pearson's chi-squared ( $\chi^2$ ) test. TLR8 allele  
1053 frequencies were compared using binary logistic regression, summarizing recessive genotypes and  
1054 adjusting for age, BMI and gender. Interaction between BCG and TLR8-A/G was assessed using  
1055 Wald's statistics. Statistical tests were performed using IBM SPSS Statistics 21 software and  
1056 figures were generated using GraphPad Prism 6 Software.

1057

1058

1059

1060 **Supplementary References**

- 1061 78. Lin, K. *et al.* MADMAX - Management and analysis database for multiple ~omics experiments. *J*  
1062 *Integr Bioinform* **8**, 160 (2011).  
1063
- 1064 79. Dai, M. *et al.* Evolving gene/transcript definitions significantly alter the interpretation of  
1065 GeneChip data. *Nucleic Acids Res* **33**, e175 (2005).  
1066
- 1067 80. Irizarry, R.A. *et al.* Exploration, normalization, and summaries of high density oligonucleotide  
1068 array probe level data. *Biostatistics* **4**, 249-264 (2003).  
1069
- 1070 81. Sartor, M.A. *et al.* Intensity-based hierarchical Bayes method improves testing for differentially  
1071 expressed genes in microarray experiments. *BMC Bioinformatics* **7**, 538 (2006).  
1072
- 1073 82. Storey, J.D. & Tibshirani, R. Statistical significance for genomewide studies. *Proc Natl Acad Sci*  
1074 *U S A* **100**, 9440-9445 (2003).  
1075
- 1076 83. Dittrich, N. *et al.* Toll-like receptor 1 variations influence susceptibility and immune response to  
1077 Mycobacterium tuberculosis. *Tuberculosis (Edinb)* **95**, 328-335 (2015)  
1078
- 1079
- 1080
- 1081
- 1082

1083 **Figure legends**

1084 **Fig. 1. Innate immune recognition of live but not dead bacteria promotes T<sub>H</sub>1 and T<sub>FH</sub>**  
1085 **differentiation.** (a) Human monocytes were stimulated with medium (ctrl), live *E. coli* (EC) or  
1086 heat killed *E. coli* (HKEC) and co-cultured with autologous naïve CD4<sup>+</sup> T cells in the presence  
1087 of SEB (TCR stimulus in all T cell conditions). Proliferation (CFSE-dilution) and cytokine  
1088 production was measured on day 5. (b) Quantification of cytokine-positive CD4<sup>+</sup> T cells. Each  
1089 dot represents an independent experiment / donor (n=9, 9, 7). (c,d) Expression of CXCR5, ICOS,  
1090 PD-1 was measured by flow cytometry (c), and quantified (d) (n=13). (e-f) Similar experiment as  
1091 in (a), expression of **BCL6** and IL-21 was measured by flow cytometry (n=9), and quantified (f).  
1092 (g) Similar experiment as in all other panels using mDC-1 as APC (n=3). (h) Quantification of  
1093 (g). (i) Expression of the indicated genes was measured in CD4<sup>+</sup> T cells at the indicated time  
1094 points by fluorescent hybridization-based multiplex assay. Results are expressed as corrected  
1095 fluorescence intensity (FI) minus FI in ctrl samples at the same time point (n=6). Error bars are  
1096 mean ± SEM (\*\*; p<0.01, \*\*\*; p<0.001; \*\*\*\*; p<0.0001).

1097

1098 **Fig. 2. De novo generated T<sub>FH</sub> cells interact with and help B cells.** (a) CD4<sup>+</sup> T cells were co-  
1099 cultured with APC as in Fig. 1a and added to autologous naïve B cells after 5 days. T<sub>FH</sub> cell markers  
1100 were measured after 12 days of sequential co-culture (n=2). (b-d) sorted CD4<sup>+</sup>CD45RA<sup>-</sup>CXCR5<sup>+</sup>  
1101 T<sub>FH</sub> cells and sorted autologous naïve CD4<sup>+</sup>CD45RA<sup>+</sup> T cells were co-cultured with tonsillar  
1102 memory B cells for 7 days and generation of CD38<sup>+</sup>CD27<sup>++</sup> plasma cells were measured (b) and  
1103 quantified (c, n= 9, 9, 3). Culture supernatants were analyzed for IgG production by ELISA (f)  
1104 (n=9, 9, 3). Error bars are mean ± SEM (\*; p<0.05, \*\*; p<0.01)

1105

1106

1107 **Fig. 3. Detection of viable bacteria induces transcriptional remodeling and skewed cytokine**  
1108 **responses in human monocytes. (a)** Human CD14<sup>+</sup>CD16<sup>-</sup> monocytes (n=4) were stimulated with  
1109 either medium (ctrl), EC or HKEC for 6h and subjected to genome wide transcriptional analysis.  
1110 Depicted is the mean signal log ratio (SLR) for each gene in EC vs ctrl treated cells plotted against  
1111 HKEC vs ctrl treated cells. Red circles indicate genes with SLR difference >2 in EC vs HKEC.  
1112 **(b)** Heat map of the 193 regulated genes with a fold change >2 or <-2 of four independent  
1113 experiments/donors. **(c)** Cytokine secretion from APC left untreated (ctrl), or stimulated with EC  
1114 or HKEC for 18h (n=3-6). **(d)** Cytokine secretion from APC stimulated with increasing  
1115 multiplicity of infection (MOI) of EC or HKEC (n=4). **(e)** Cytokine secretion from APC stimulated  
1116 with live or heat killed *B. subtilis* (BS and HKBS respectively, upper panel, n=2-5), and live or  
1117 heat killed *M. bovis* strain *BCG* (BCG and HKBCG respectively, lower panel, n=4) **(f)** APC were  
1118 treated as in (c) and surface expression of the indicated markers was measured by flow cytometry  
1119 at 18h post infection (n=5). Error bars are mean ± SEM (\*; p<0.05, \*\*; p<0.01, \*\*\*; p<0.001)

1120

1121 **Fig. 4. ‘Viability-induced’ IL-12 production is a critical signal for T<sub>FH</sub> differentiation. (a,b)**  
1122 CD4<sup>+</sup> T cells were polyclonally activated by plate-bound anti-CD3 and soluble anti-CD28  
1123 antibodies in the presence of supernatants collected from APC stimulated for 18h with ctrl, EC or  
1124 HKEC. Cytokine production was measured by flow cytometry (a, n=19, 8) and ELISA (b, n=11).  
1125 **(c)** Linear regression analysis of IL-21 production by CD4<sup>+</sup> T cells and the indicated cytokines in  
1126 APC supernatants (n=45, 21, 21). **(d-g)** T cells were cultured as in a-c in the presence of the  
1127 indicated neutralizing antibodies or recombinant cytokines ( $\alpha$ IL-12; anti-IL-12 antibody etc., rIL-  
1128 12: recombinant IL-12 etc.). IL-21 and **BCL6** expression were measured by flow cytometry (d,e)  
1129 (n=8), IL-21 production was quantified by ELISA (f, g) (n=7). Error bars are mean ± SEM (\*;  
1130 p<0.05, \*\*; p<0.01, \*\*\*; p<0.001).

1131

1132

1133 **Fig. 5. APC sense live bacteria via TLR8.** (a) Monocytes treated as indicated ('2'; ligand for  
1134 TLR2 etc.), cytokine production was measured by ELISA (n=2). (b) Monocytes were stimulated  
1135 as indicated (pLA= polycationic polypeptide poly-l-arginine (*pLa*), RNA= bacterial RNA) and  
1136 cytokine production was measured by ELISA (n=3, 4, 4). (c-d) Cytokine release from primary  
1137 human monocytes treated with siRNA against TLR8 (c) and MyD88 (d) or control siRNA (ctrl)  
1138 and stimulated as indicated (n=3). #; not detectable. Error bars are mean  $\pm$  SEM. (\*\*; p<0.01, \*\*\*;  
1139 p<0.001)

1140

1141 **Fig. 6. TLR8 is crucial in the detection of viable bacteria and subsequent instruction of T<sub>FH</sub>**  
1142 **responses.** (a-b) CD4<sup>+</sup> T cells were stimulated in the presence of culture supernatants from APC  
1143 previously stimulated with live or killed bacteria, or the indicated TLR ligands. IL-21 and **BCL6**  
1144 expression were detected by flow cytometry (n=7). (b) Quantification of (a). (c) APC were  
1145 stimulated with live or killed bacteria, the TLR8 agonist CL075 (0.1, 0.5 and 1 $\mu$ g/ml respectively),  
1146 MPLA (0.1, 0.5 and 1 $\mu$ g/ml respectively), or CpG (0.1, 1 and 2.5 $\mu$ M respectively), and  
1147 subsequently co-cultured with CD4<sup>+</sup> T cells as in Figure 1. **BCL6**/IL-21 expression was detected  
1148 by flow cytometry (n=7). (d-e) APC were stimulated with live or killed bacteria, and/or with  
1149 bacterial RNA complexed with pLa, and supernatants were used to stimulate CD4<sup>+</sup> T cells as in  
1150 (a). **BCL6**/IL-21 expression was detected by flow cytometry and IL-21 production was measured  
1151 by ELISA (n=4). (f-g) CD4<sup>+</sup> T cells were stimulated in the presence of culture supernatants from  
1152 siRNA-treated APC (n=8). IL-21/**BCL6** co-expression was measured by flow cytometry (f, g left  
1153 panel) and IL-21 production was measured by ELISA (g, right panel). Error bars are mean  $\pm$  SEM.  
1154 (\*; p<0.05, \*\*; p<0.01, \*\*\*; p<0.001).

1155

1156

1157 **Fig. 7. Detection of viable bacteria in porcine APC promotes T<sub>FH</sub> differentiation. (a, b)**  
1158 Porcine CD14<sup>+</sup>CD172<sup>+</sup> monocytes (a) and CD14<sup>+</sup>CD172<sup>+</sup> DC (b) were sorted from spleen samples  
1159 and stimulated with medium (ctrl), EC, HKEC, live attenuated *S. enterica* serovar Typhimurium  
1160 vaccine (ST), heat killed ST (HKST) or with CL075. IL-12p40 and IL-6 was measured by  
1161 multiplex bead array (n=3). (c) Cytokine release from porcine splenic CD14<sup>+</sup> monocytes treated  
1162 with siRNA against porcine TLR8 or control siRNA (ctrl), and stimulated as indicated (n=3). (d)  
1163 Porcine splenocytes were stimulated with ConA in the presence of increasing doses of ST or  
1164 HKST. BCL6/IL-21 expression was measured in CD4<sup>+</sup> T cells by flow cytometry on day 4. (e)  
1165 Quantification of (d, n=3). (f) Porcine splenocytes were stimulated with CL075, LPS, or bacterial  
1166 RNA (RNA + pLA) in the presence of ConA. BCL6/IL-21 expression was measured in CD4<sup>+</sup> T  
1167 cells on day 4 (n=3). Error bars are mean ± SEM. (n.s.; not significant, \*, p<0.05, \*\*, p<0.01, \*\*\*,  
1168 p<0.001).

1169

1170 **Fig. 8 A live attenuated vaccine promotes T<sub>FH</sub> differentiation *in vivo*. (a)** Five week old  
1171 domestic piglets were vaccinated subcutaneously with ST, HKST or saline (ctrl), and BCL6/IL-21  
1172 expressing CD4<sup>+</sup> T cells were measured in draining lymph nodes (LN) or spleens on day 30 after  
1173 immunization (n=5/group). (b) Quantification of (a). (c) Sections of paraffin embedded spleen  
1174 tissues were stained for PAX5. Scale bars: upper panels = 5 mm; lower panels = 500 µm. (d)  
1175 morphometric quantification of PAX5<sup>+</sup> follicles spleen sections tissue represented in (c). (e) Co-  
1176 immunofluorescence staining of PAX5 (red) and KI67 (green) on spleen section of pigs  
1177 vaccinated with ST. The cell nuclei were stained with DAPI (blue). Scale bar = 50 µm. (f)  
1178 Antibody forming cells (AFC) / plasma cells (PC) were measured by flow cytometry in spleen  
1179 samples (n= 4/group). (g) anti-*Salmonella* IgG was measured by ELISA in serum samples taken  
1180 before vaccination (day 0), and on day 14 and 21 post-vaccination. Error bars are mean ± SEM.  
1181 (\*; p<0.05, \*\*; p<0.01).

1182

1183



1184 **Fig. 9. Association of a TLR8 SNP with BCG-induced immunity.** (a) TLR8-A and TLR-G  
1185 allele distribution in 458 subjects (293 cases of confirmed TB and 165 household contacts =  
1186 controls) (left panel), and 345 subjects (180 cases of confirmed pulmonary TB (PTB) and 165  
1187 controls) (right panel). (b) TLR8-A and TLR8-G allele distribution in BCG-vaccinated (upper  
1188 panel) and unvaccinated (lower panel) PTB cases and controls, one individual was excluded from  
1189 the analysis due to unclear vaccination status. (c) Odds ratio (OR [CI95%], adjusted for sex, age  
1190 and BMI) for PTB in BCG vaccinated versus unvaccinated subjects calculated for the whole study  
1191 population and separately for each TLR8 genotype (bars represent OR, error bars represent CI  
1192 95%). ORs differ significantly between TLR8-A and TLR8-G as calculated by Wald's test. (\*;  
1193  $p < 0.05$ , \*\*;  $p < 0.01$ ).

Fig. 1

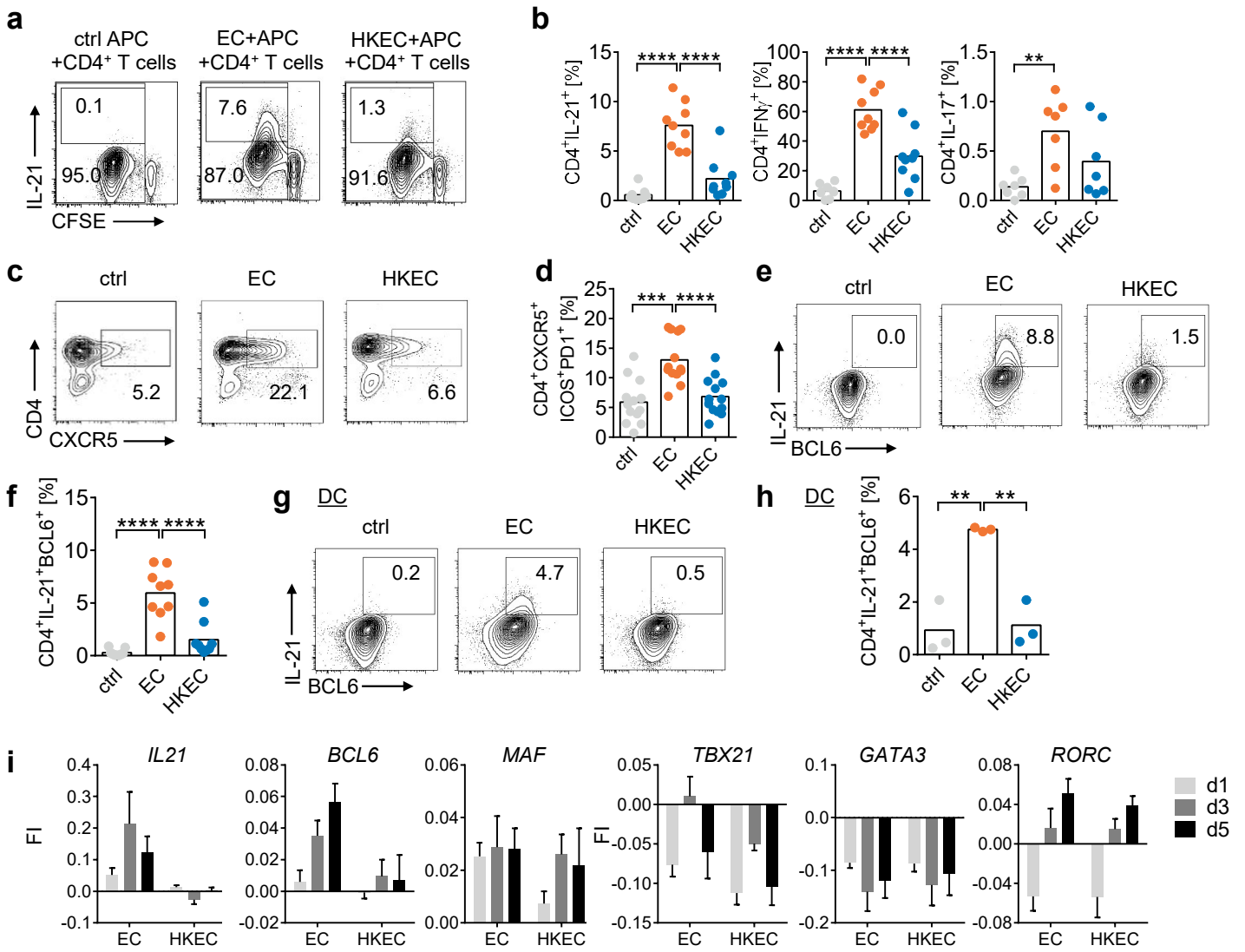


Fig. 2

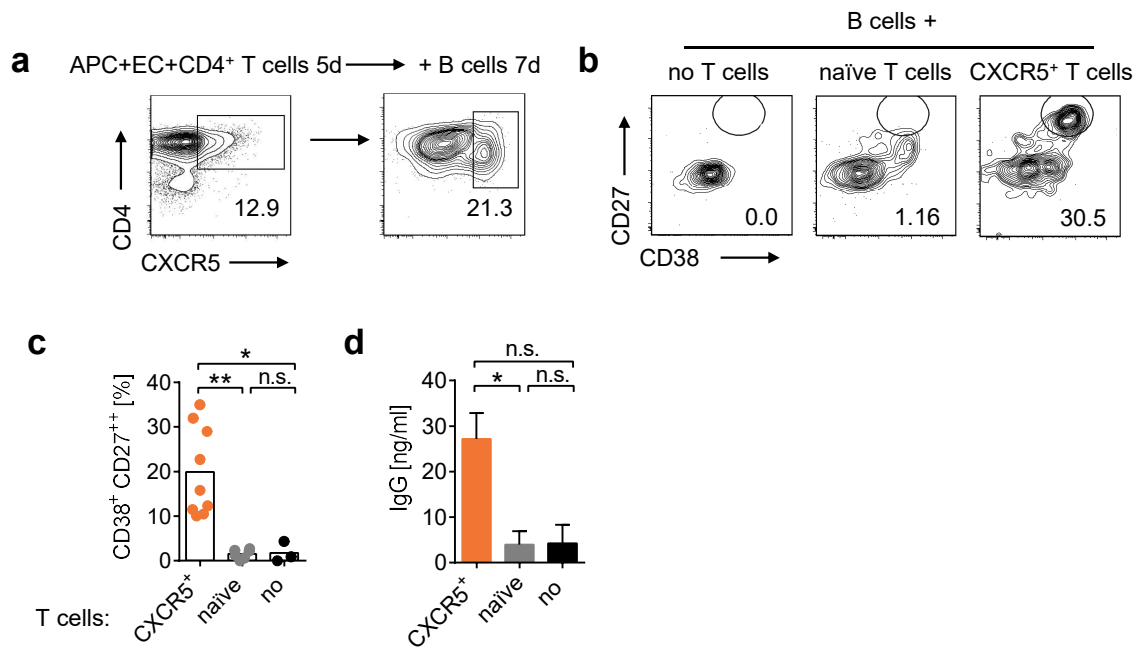


Fig. 3

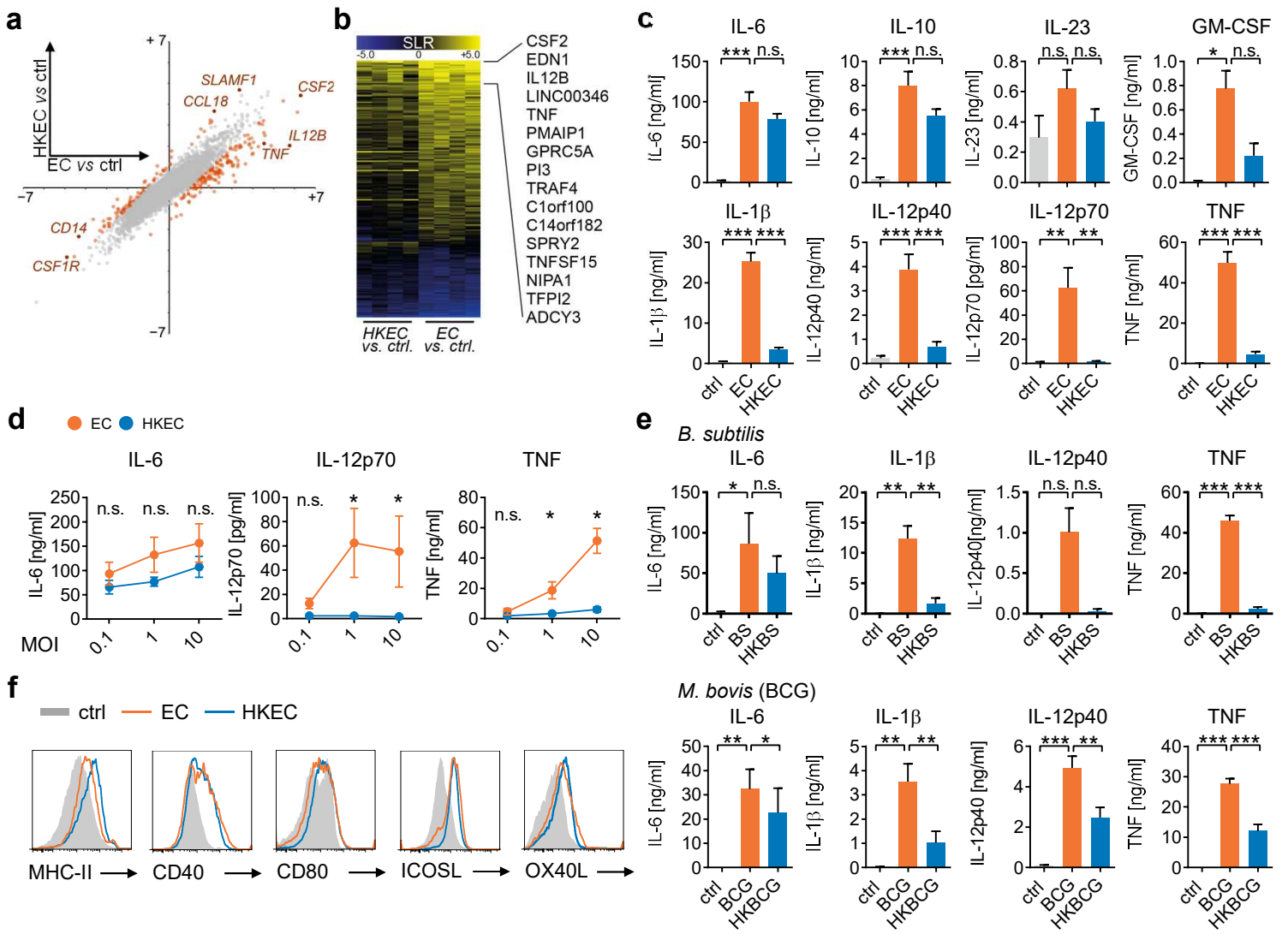


Fig. 4

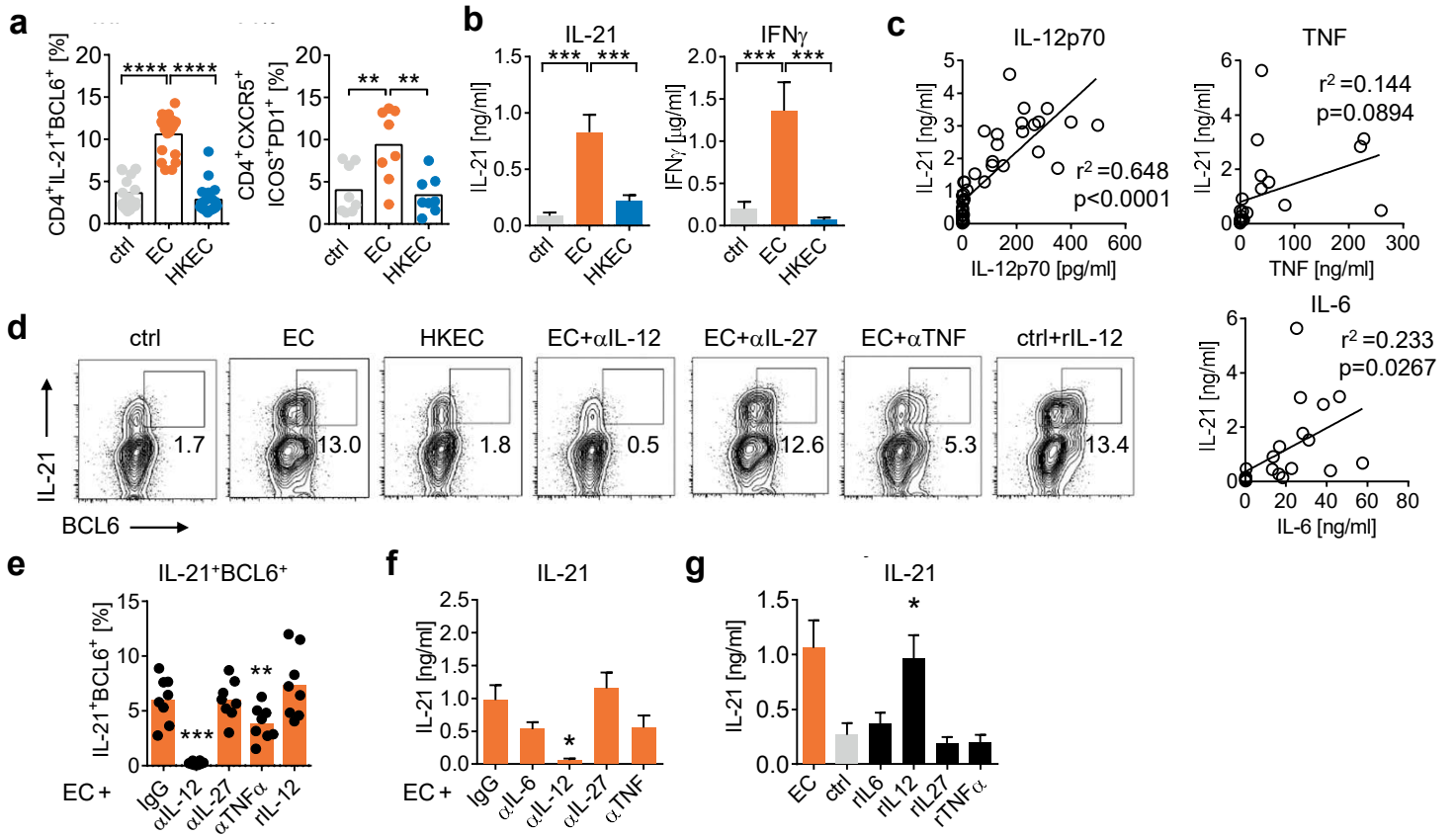


Fig. 5

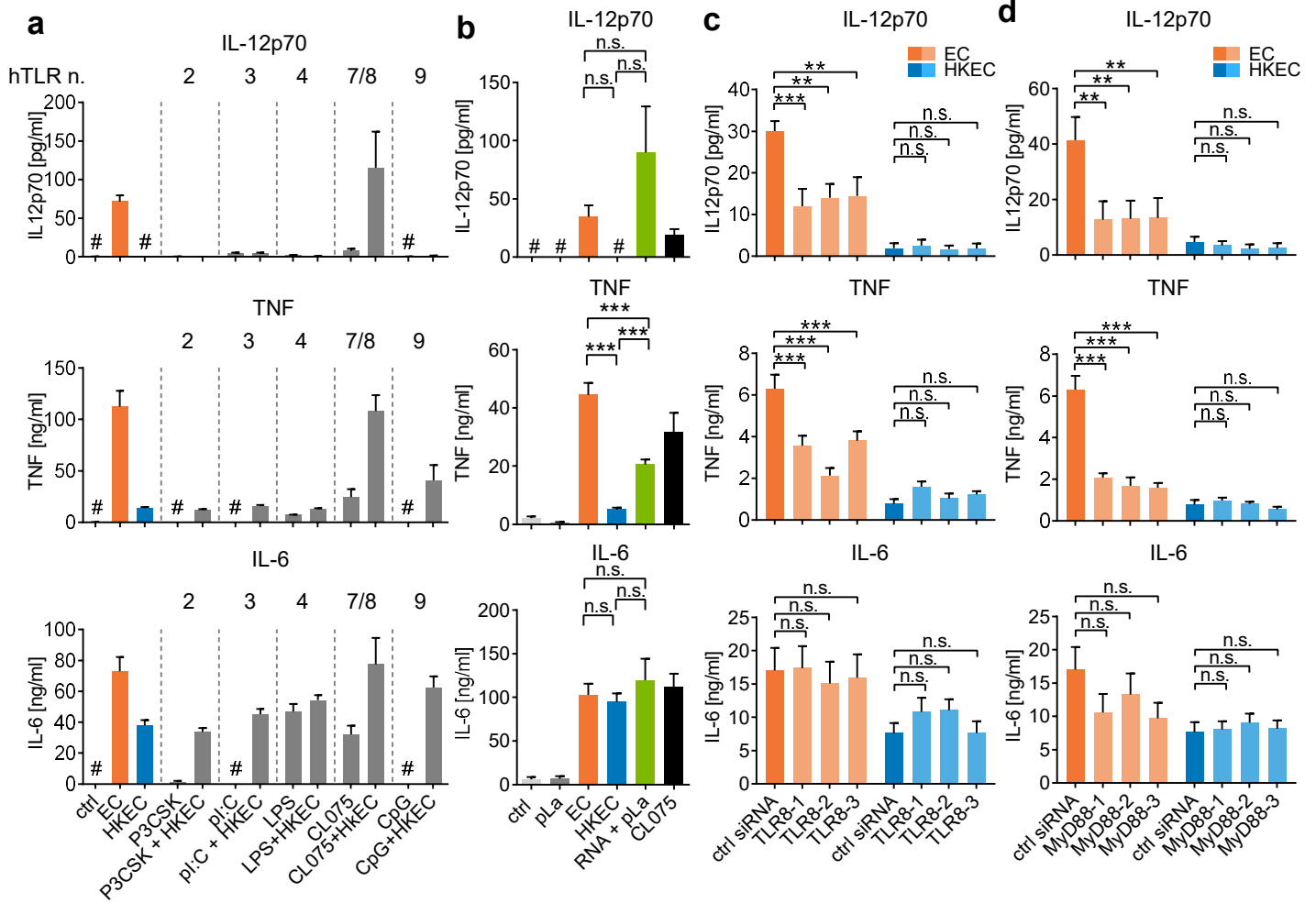


Fig. 6

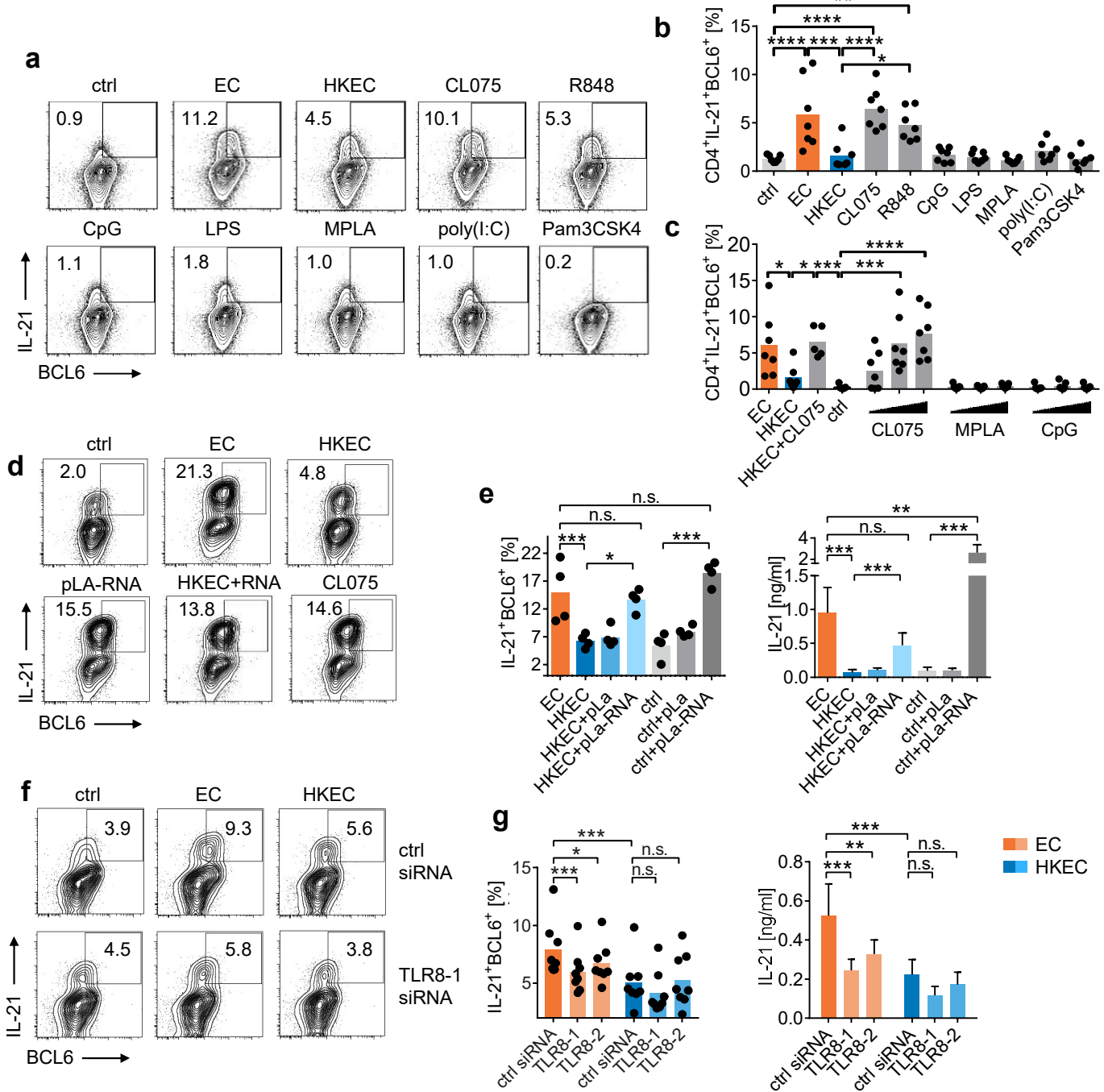


Fig. 7

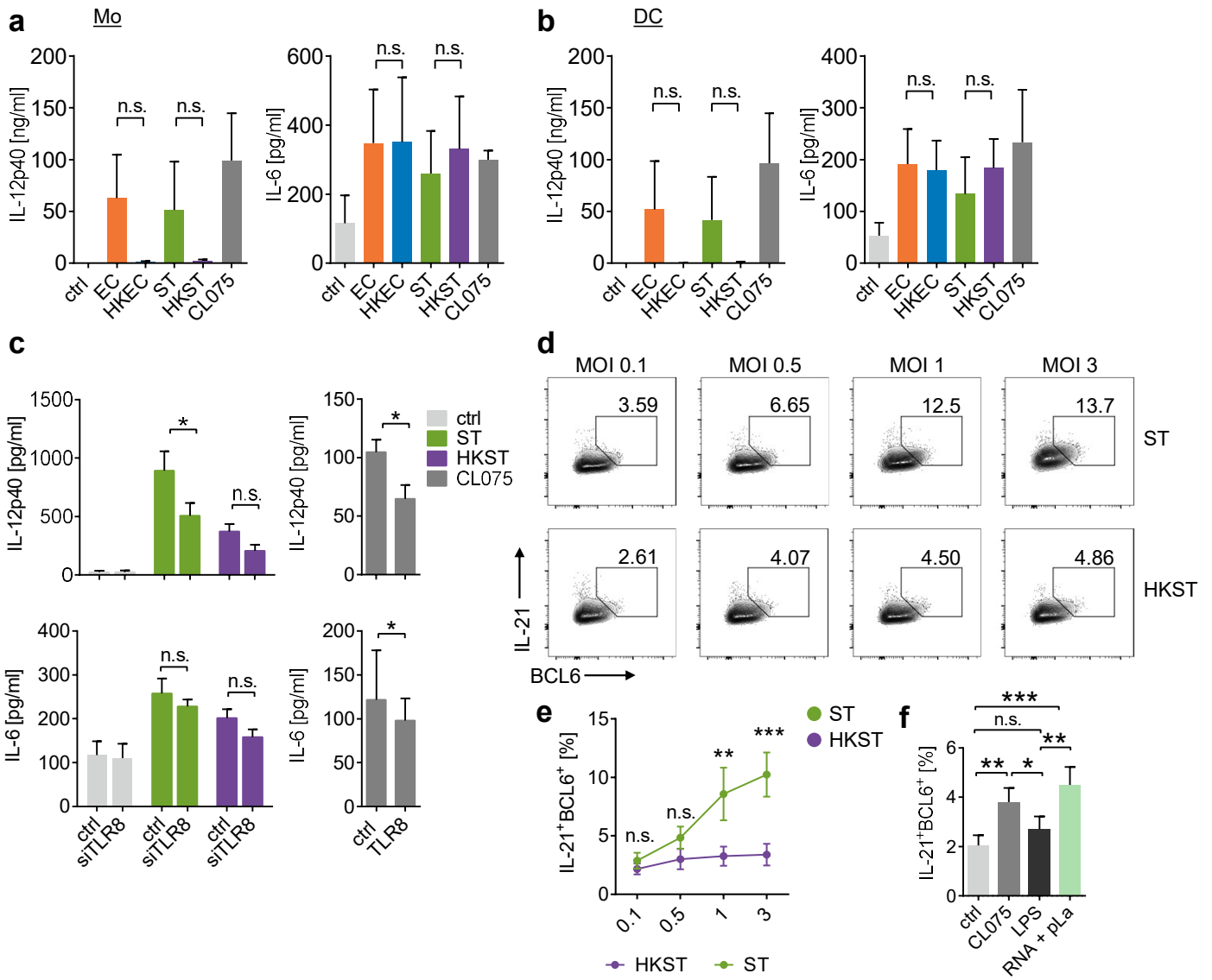




Fig. 8

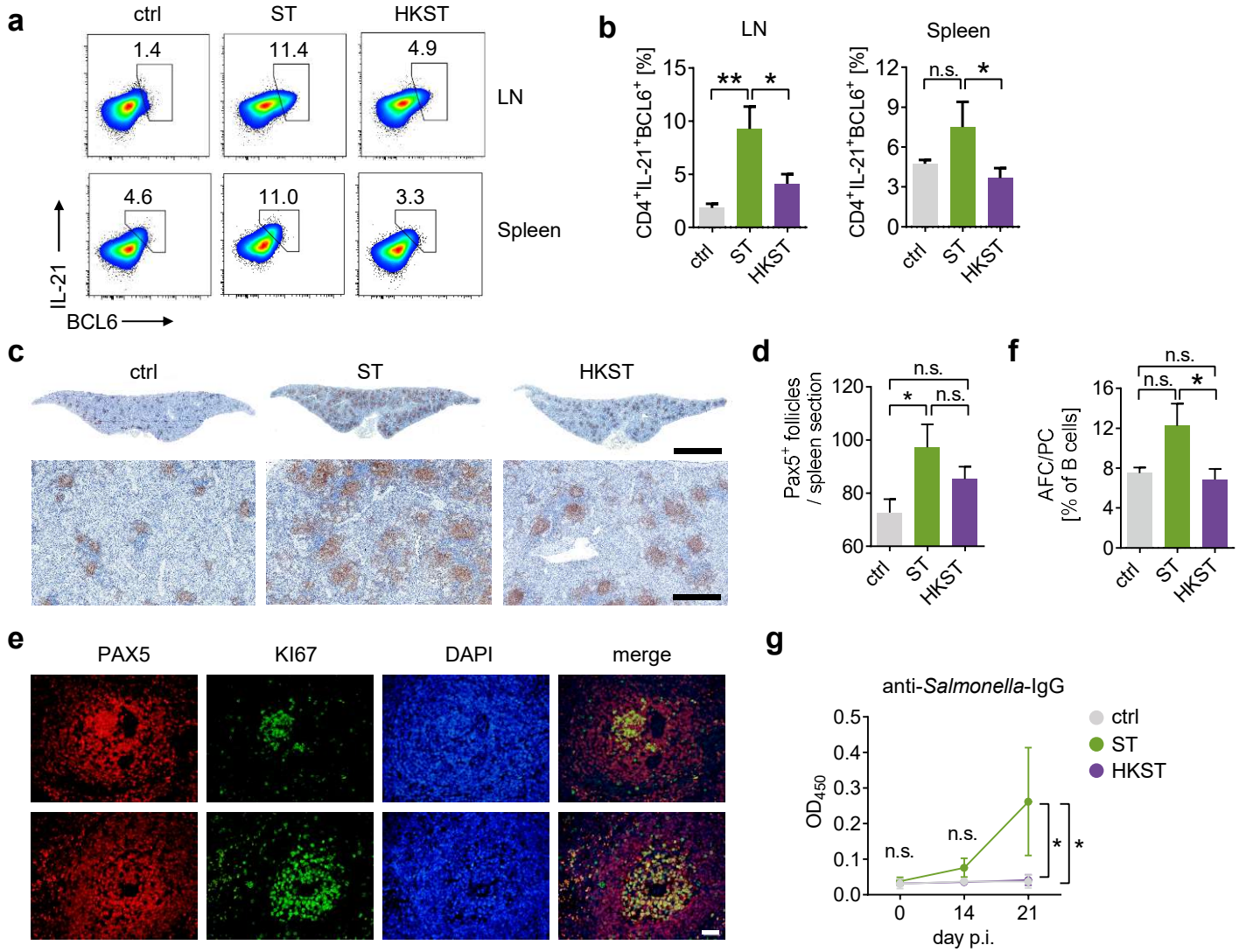


Fig. 9

